

Air Force Institute of Technology

AFIT Scholar

Theses and Dissertations

Student Graduate Works

12-2004

The Kinetics Following Photolysis of Nitrosyl Bromide

Lori A. Mahoney

Follow this and additional works at: <https://scholar.afit.edu/etd>



Part of the [Plasma and Beam Physics Commons](#)

Recommended Citation

Mahoney, Lori A., "The Kinetics Following Photolysis of Nitrosyl Bromide" (2004). *Theses and Dissertations*. 3719.

<https://scholar.afit.edu/etd/3719>

This Thesis is brought to you for free and open access by the Student Graduate Works at AFIT Scholar. It has been accepted for inclusion in Theses and Dissertations by an authorized administrator of AFIT Scholar. For more information, please contact richard.mansfield@afit.edu.



**THE KINETICS FOLLOWING PHOTOLYSIS
OF NITROSYL BROMIDE**

THESIS

Lori A. Mahoney, Civilian

AFIT/GAP/ENP/04-07

**DEPARTMENT OF THE AIR FORCE
AIR UNIVERSITY**

AIR FORCE INSTITUTE OF TECHNOLOGY

Wright-Patterson Air Force Base, Ohio

APPROVED FOR PUBLIC RELEASE; DISTRIBUTION UNLIMITED

The views expressed in this thesis are those of the author and do not reflect the official policy or position of the United States Air Force, Department of Defense, or the United States Government.

AFIT/GAP/ENP/04-07

THE KINETICS FOLLOWING PHOTOLYSIS OF NITROSYL BROMIDE

THESIS

Presented to the Faculty

Department of Engineering Physics

Graduate School of Engineering and Management

Air Force Institute of Technology

Air University

Air Education and Training Command

In Partial Fulfillment of the Requirements for the

Degree of Master of Science in Applied Physics

Lori A. Mahoney, BS

Civilian

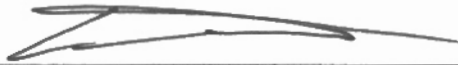
December 2004

APPROVED FOR PUBLIC RELEASE; DISTRIBUTION UNLIMITED.

THE KINETICS FOLLOWING PHOTOLYSIS OF NITROSYL BROMIDE

Lori A. Mahoney, BS
Civilian

Approved:



Glen P. Perram (Chairman)

16 Nov 04

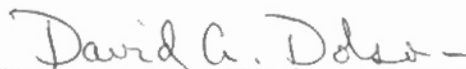
date



William F. Bailey (Member)

16 Nov 2004

date



David A. Dolson (Member)

11/16/04

date

Abstract

One candidate for the development of a tunable laser in the mid-infrared for use as a defensive countermeasure against passive sensors exploits the nitric oxide (NO) transition at 5.4 μm . However, the difficulty with this mechanism is that when bromine (Br_2) and NO are present in a mixture, nitrosyl bromide (BrNO) is also created. The absorption bands present in BrNO complicate the design of such a laser. This thesis determines the forward and reverse rate constants of the reaction of Br_2 and NO to form BrNO following the photolysis of BrNO using Fourier Transform Infrared absorption spectroscopy. Other studies have been conducted to determine both the forward and reverse reaction rate constants using different methods, however some of the methods used create uncertainty in the results.

In this effort samples with a total pressure of 10.0 torr were used containing either bromine or nitric oxide in excess. The use of Br_2 versus NO as the excess reagent has an effect on which mechanism can be used to describe the reaction, but does not affect the reaction rate constants. When NO is the excess reagent, the reaction obeys pseudo first-order kinetics, where the reverse reaction does not significantly impact the overall reaction. This is not true when Br_2 is the excess reagent. In both cases, third-order kinetics accurately describe the $\text{Br}_2 + 2\text{NO} \leftrightarrow 2\text{BrNO}$ reaction giving a forward reaction rate constant of $k_f = 1.56 \pm 0.20 \times 10^{-38} \text{ cm}^6/\text{molecule}^2\text{-s}$ at $293 \pm 1 \text{ K}$. The reverse rate constant was calculated as $k_r = 2.29 \pm 0.33 \times 10^{-21} \text{ cm}^3/\text{molecule-s}$ and the equilibrium constant as $K_{\text{eq}} = 171 \pm 13 \text{ atm}^{-1}$. This result is consistent with previous results.

Acknowledgments

The assistance and encouragement of many people helped me to finish this research project. As they have for so many students, the AFIT lab technicians provided wonderful support and expertise. I need to thank Greg Smith and Mike Ranft especially for spending their valuable time directing me through the processes used in the setup and execution of this experiment.

I would like to express my sincere appreciation to my faculty advisor, Dr. Glen Perram, for his patience and guidance throughout the course of this thesis effort. The insight and experience was greatly appreciated. I am also indebted to Major Pat Kee for helping point me in the right direction at the beginning of this project.

Much of this research project and all of my class work at AFIT was performed while I was working full-time at the National Air and Space Intelligence Center. Without the understanding and support of my various supervisors there, I would have never been able to start, much less finish, this effort.

Finally, I am very grateful to my husband for his encouragement and emotional support throughout this entire project. He helped me keep going when it would have been much easier to call it quits.

Lori Mahoney

Table of Contents

	Page
Abstract	iv
Acknowledgments	v
List of Figures	vii
List of Tables	ix
I. Introduction	1
Problem Statement.....	1
Previous Results	2
II. Theory	4
BrNO Spectrum	4
Kinetics Reactions	5
III. Experimental Procedure	12
Experimental Set Up.....	12
Photodissociation and Reformation of BrNO.....	15
Collection of Spectra	16
Safety Precautions	17
IV. Results	18
Third-Order Solution	18
First-Order Solution.....	24
Solution Near Zero BrNO Concentration	25
Error.....	27
V. Conclusions	29
Appendix A. Detailed Calculation of the Kinetics Equations	30
Appendix B. Kinetics Data Obtained from FTIR spectra	35
Appendix C. Detailed Calculations of k_f , k_r , K_{eq} values.....	43
Bibliography	45

List of Figures

Figure	Page
1. Composite 2 cm^{-1} resolution transmittance spectrum of ν_1 vibrational band of BrNO measured at various concentrations of BrNO.	4
2. Representative sample of measured 2 cm^{-1} resolution FTIR transmittance data	7
3. Solution to third-order kinetics problem.....	10
4. Gas handling vacuum system used to fill the glass cell	13
5. Pressure decrease over time due to loss of Br_2	14
6. Apparatus used to collect kinetics data.....	15
7. Simplified schematic of the MB 157 FTIR Spectrometer	16
8. Example of area measured “under” the BrNO $\nu=1$ line.....	18
9. Example of normalized BrNO concentration, x , as a function of time, t	19
10. Example of third-order solution fit ($r^2 = 0.952$) to observed data with K_2 as the only fit parameter.....	20
11. Example of first-order solution fit ($r^2 = 0.997$) to observed data with $A=K_1\alpha^2$ and C_1 as fit parameters	25
12. Example of concentration versus time near $[\text{BrNO}]_t$ equals zero	26
13. Normalized BrNO concentration, x , plotted as a function of time, t , for sample 1	35
14. Normalized BrNO concentration, x , plotted as a function of time, t , for sample 2	36
15. Normalized BrNO concentration, x , plotted as a function of time, t , for sample 3	36
16. Normalized BrNO concentration, x , plotted as a function of time, t , for sample 4	37
17. Normalized BrNO concentration, x , plotted as a function of time, t , for sample 5	37
18. Normalized BrNO concentration, x , plotted as a function of time, t , for sample 6	38
19. Normalized BrNO concentration, x , plotted as a function of time, t , for sample 7	38
20. Normalized BrNO concentration, x , plotted as a function of time, t , for sample 8	39
21. Normalized BrNO concentration, x , plotted as a function of time, t , for sample 9	39

22. Normalized BrNO concentration, x, plotted as a function of time, t, for sample 10	40
23. Normalized BrNO concentration, x, plotted as a function of time, t, for sample 11	40
24. Normalized BrNO concentration, x, plotted as a function of time, t, for sample 12	41
25. Normalized BrNO concentration, x, plotted as a function of time, t, for sample 13	41
26. Normalized BrNO concentration, x, plotted as a function of time, t, for sample 14	42
27. Normalized BrNO concentration, x, plotted as a function of time, t, for sample 15	42

List of Tables

Table	Page
1. Band centers (cm^{-1}) of BrNO	5
2. Example of calculation of $[\text{Br}_2]_0$ and $[\text{NO}]_0$ from the curve fit data	21
3. Summary of partial pressures at the start of data collection	21
4. Calculated k_f and k_r values using data fit to third-order solution with K_2 as only fit parameter	22
5. Calculated k_f and k_r values using data fit to third-order solution with K_2 and K_2 as fit parameters	23
6. Values of k_f , k_r , and K_{eq} obtained in this and previous efforts	23
7. Calculated k_f and k_r values using data fit to first-order solution with $A=K_1\alpha^2$ and C_1 as fit parameters	24
8. Measured versus calculated slope near $[\text{BrNO}]_t = 0$	26
9. Values used to determine k_f and k_r for case where K_2 was the only fit parameter	43
10. Values used to determine k_f , k_r and K_{eq} for case where K_1 and K_2 were the fit parameters	44
11. Values used to determine k_f and k_r for case where $K_1\alpha^2$ was the fit parameter	44

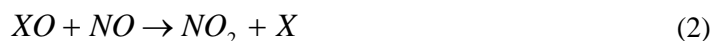
THE KINETICS FOLLOWING PHOTOLYSIS OF NITROSYL BROMIDE

I. Introduction

Problem Statement

One candidate for the development of a tunable laser in the mid-infrared for use as a defensive countermeasure against passive sensors exploits the nitric oxide (NO) transition at 5.4 μm .¹¹ This system utilizes the photolysis of an electronically excited bromine atom (Br^*) which collisionally transfers energy to $\text{NO}_{v=2}$, the receptor molecule. This excited molecule relaxes back to the ground state via radiation, forming the laser. The rotational distribution within the excited vibrational states provides a tunable range of approximately 1 micron.⁶ The Br^* in this system is produced by the photolysis of molecular bromine (Br_2).¹¹ However, the difficulty with this mechanism is that when Br_2 and NO are present in a mixture, nitrosyl bromide (BrNO) is also created. The absorption bands present in BrNO complicate the design of such a laser. The kinetics reported here help to increase our understanding of the chemical reactions involved in the production and destruction of BrNO .

Additionally, halogens, including Br_2 , have been linked to chemical reactions believed to describe the ozone depletion cycle. Chlorofluorocarbons contain halogens that deplete the ozone through the reactions



where X represents fluorine, chlorine, iodine or bromine. The net reaction reduces the ozone

concentration.



The halogen atom is not consumed in these reactions and may react with nitric oxide and a third body, Y, to form a nitrosyl halide



The halogen atoms also form diatomic molecules that react with the NO again, forming additional nitrosyl halides



If the halogen is present only as X_2 or XNO , versus X , molecules it cannot aid in the depletion of ozone. A thorough understanding of the kinetics of the reactions is required to determine the effects of these processes.⁴ This thesis addresses some of the chemical kinetic issues present when a halogen reacts with nitric oxide.

Previous Results

Previous works studied the reaction of halogens, specifically bromine, with nitric oxide, however some of the methods used cause uncertainty in the results. Hisatsune and Zafonte determined the forward and reverse reaction rate constants from the reaction of $BrNO$, NO and Br_2 by mixing NO and Br_2 and following the time dependence of the strong NO stretch infrared absorption band of the product $BrNO$.⁸ Using the equilibrium state of Br_2 , NO and $BrNO$, Houel and van den Bergh determined the UV/visible absorption spectrum of $BrNO$.¹⁰ Hippler studied the recombination of Br atoms after photolysis of less than 0.3 torr of Br_2 at room temperature, in the range of 1-100 atm of the inert diluent helium. He also studied the

recombination of Br and NO in the presence of helium.⁷ Godfrey examined the kinetics of BrNO formation and destruction using time-resolved photolysis techniques. The kinetic mechanism and rates for the photolysis of the BrNO mixture were also examined and validated for total pressures ranging from 28-111 torr.⁴ Only Godfrey included the effect of the loss of Br₂ to the internal surfaces of the cell in the calculation of the reaction rate constants. The previously determined reaction rates range from 1.32 ± 0.14 to $1.68 \pm 0.11 \times 10^{-38}$ cm⁶/molecule²-s for k_f and from 2.09 ± 0.55 to 3.71×10^{-21} cm³/molecule-s for k_r.

II. Theory

BrNO Spectrum

The fundamental vibrational band centers of BrNO exist at 1798.7 cm^{-1} for the ν_1 band, 542.0 cm^{-1} for the ν_2 band, and 266.4 cm^{-1} for the ν_3 band.¹³ The ν_1 band is primarily due to an NO bond stretch while ν_2 and ν_3 are predominantly mixes of NBr stretch and angle bending. The ν_1 fundamental band of the two main isotopomers of BrNO ($^{79}\text{BrNO}$ and $^{81}\text{BrNO}$) is the strongest band in the infrared spectrum. The ν_1 band is of parallel structure with only A-type transitions. The P and R branches are dominant, but weaker Q-branch features also appear as a shoulder on the P branch. The line density of the spectrum is very high, due to the small values of the rotational constants B and C and the presence of two equally abundant isotopomers.³

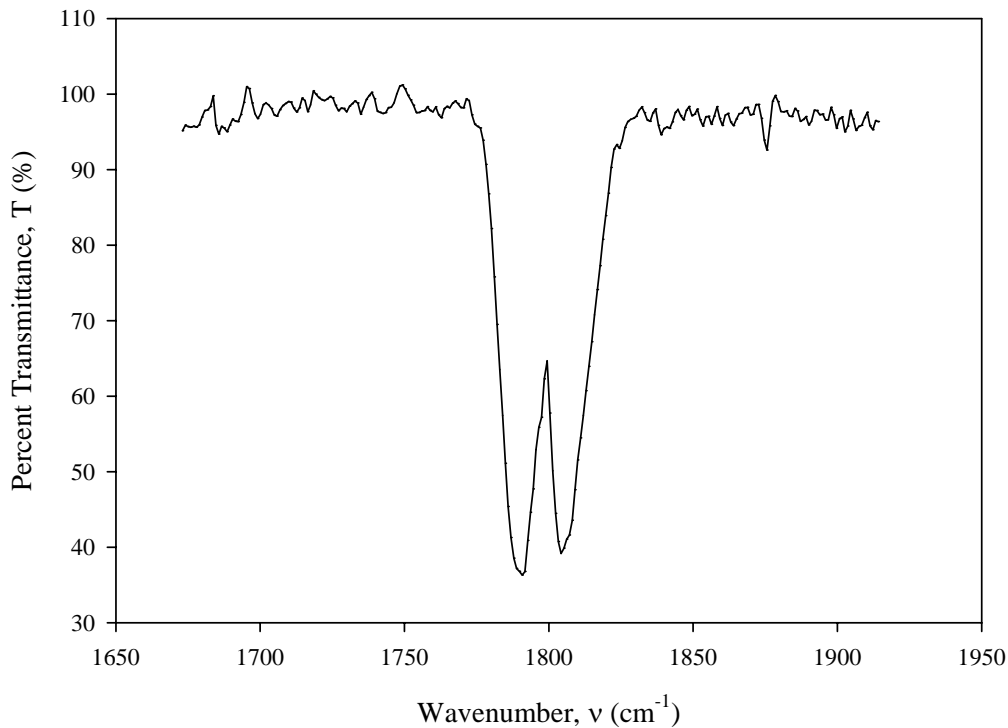


Figure 1. Composite 2 cm^{-1} resolution transmittance spectrum of ν_1 vibrational band of BrNO measured at various concentrations of BrNO.

Table 1. Band centers (cm⁻¹) of BrNO^{3,13}

	⁷⁹ Br ¹⁴ N ¹⁶ O	⁸¹ Br ¹⁴ N ¹⁶ O	Br ¹⁵ N ¹⁶ O	Br ¹⁴ N ¹⁸ O	Br ¹⁵ N ¹⁸ O	Relative Intensity
v ₁	1798.751	1798.742	1768.3	1751.5	1719.5	VVVS
v ₂	542.0		527.8	No Data	521.5	VS
v ₃	266.2		264	No Data	257.0	S

Kinetics Reactions

BrNO photodissociates into Br₂ and NO when it is illuminated with a visible wavelength laser light source. After the light is removed the Br₂ and NO naturally recombine, at a rate k_f, to form BrNO, while a backwards reaction regenerates Br₂ and NO, until an equilibrium concentration, K_{eq}, is reached, with any excess Br₂ or NO remaining in the mixture.



The rate of change of the concentration of BrNO over time is described by

$$\frac{d[BrNO]_t}{dt} = -k_p [BrNO]_t I_p - k_1 [Br]_t [BrNO]_t + 2k_f [NO]_t^2 [Br_2]_t - 2k_r [BrNO]_t^2 \quad (10)$$

The calculation of the forward and reverse reaction rate constants in equation (9) can be simplified by considering only the data collected after the light source has been shut off, where I_p=0, and the BrNO mixture is returning to equilibrium. The second term in equation (10) is

eliminated because [Br] exists for less than a microsecond making k_1 negligible when compared to k_f and k_r . This reaction is still third-order and the rate of change of BrNO over time is

$$\frac{d[BrNO]_t}{dt} = 2k_f [NO]_t^2 [Br_2]_t - 2k_r [BrNO]_t^2 \quad (11)$$

Third-order bond-breaking reactions between stable molecules are quite rare and all known examples involve nitric oxide as one of the reactants.¹⁴ The best understood reactions are those involving chlorine and oxygen. The collision of three molecules is so unlikely that many scientists believe the reaction consists of two steps. However, no experiment has ever provided evidence for the existence of any intermediate complex.⁸

The normalized concentration of BrNO, which is defined as x , can be calculated from the FTIR spectroscopy data collected for each sample by measuring at time, t , and at equilibrium, the area under the curve of the BrNO ($\nu=1$) band.

$$x \equiv \frac{[BrNO]_t}{[BrNO]_{eq}} \quad (12)$$

The Beer-Lambert Law describes the absorption, A , of radiation by molecules after passing through a length, l , of gas, such as during FTIR spectroscopy, as

$$A = \log_{10} \left(\frac{I}{I_0} \right) = -\epsilon cl$$

or

$$A = \log_{10} \left(\frac{I}{I_0} \right) = \frac{-\sigma [BrNO] l}{\ln(10)} \quad (13)$$

where the I is the intensity of the beam passing through the filled cell, I_0 is the intensity detected when the cell is empty, c is the concentration in mol/liter, $[\text{BrNO}]$ is the concentration of BrNO in molecules/cm³, ϵ is the absorption coefficient in liter/mole-cm, σ is the absorption cross section in cm², and l is in centimeters.⁹ Since σ and l are constant, the Beer-Lambert Law can be used to determine that the ratio of areas under the absorption or transmittance curve for a specific peak taken at two different times during the reaction is equal to the ratio of the concentrations of the sample at those times.

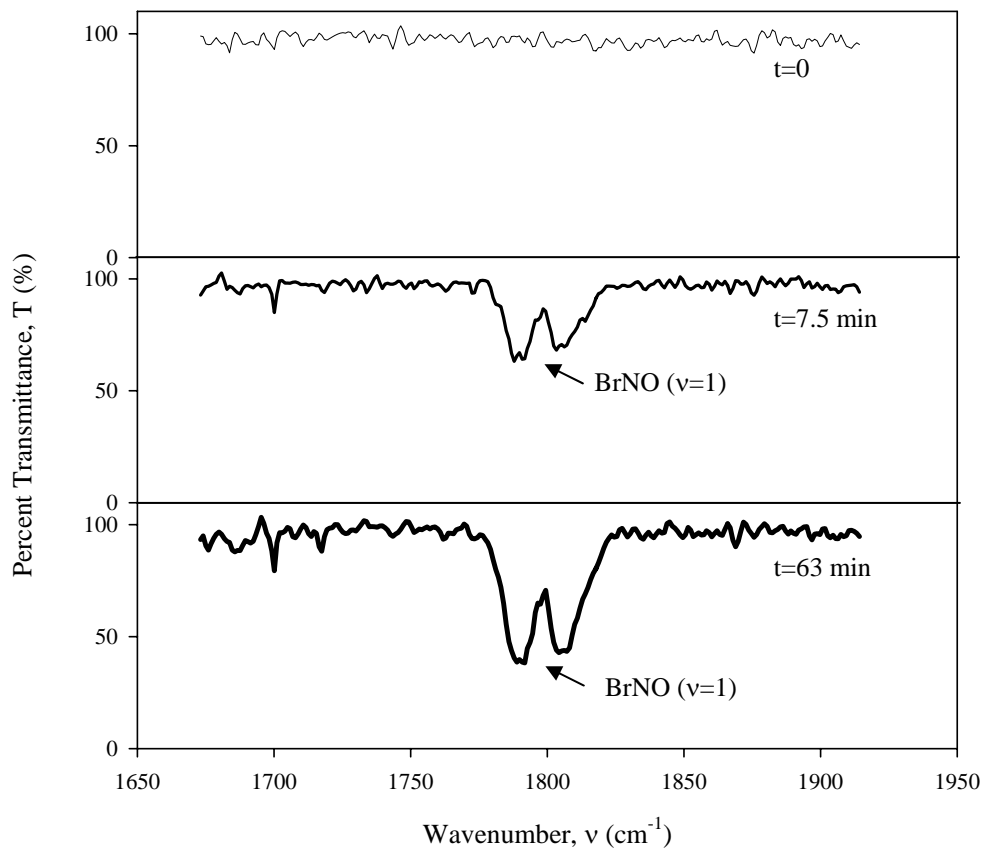


Figure 2. Representative sample of measured 2 cm⁻¹ resolution FTIR transmittance data at time = 0, time = 7.5 min, and t = 63 min (equilibrium). $P_0(\text{Br}_2) = 0.25$ torr, $P_0(\text{NO}) = 9.75$ torr, $P_0(\text{BrNO}) = 0$ torr.

The molecular concentrations for Br₂, NO, and BrNO at equilibrium are

$$[Br_2]_{eq} = [Br_2]_0 - n_{eq} \quad (14)$$

$$[NO]_{eq} = [NO]_0 - 2n_{eq} \quad (15)$$

$$[BrNO]_{eq} = [BrNO]_0 + 2n_{eq} \quad (16)$$

where n_{eq} is a constant used to determine the equilibrium concentration of each species in the sample. By substituting equations (14), (15), and (16) into the equation for the equilibrium constant,

$$K_{eq} = \frac{k_f}{k_r} = \frac{[BrNO]_{eq}^2}{[NO]_{eq}^2 [Br_2]_{eq}} \quad (17)$$

a value for n_{eq} can be found from the initial concentrations of Br₂, NO, and BrNO. Since $[BrNO]_0 = 0$, the value for n_{eq} is calculated from

$$K_{eq} = \frac{4n_{eq}^2}{([Br_2]_0 - n_{eq})([NO]_0 - 2n_{eq})^2} \quad (18)$$

Additionally, the concentrations of Br₂, NO, and BrNO at time, t, in terms of x are

$$[BrNO]_t = x[BrNO]_{eq} \quad (19)$$

$$[NO]_t = [NO]_{eq} + [BrNO]_{eq}(1-x) \quad (20)$$

$$[Br_2]_t = [Br_2]_{eq} + \frac{1}{2}[BrNO]_{eq}(1-x) \quad (21)$$

Substituting these values into equation (11) gives

$$\frac{dx}{dt} = 2k_f [BrNO]_{eq}^2 \left(\frac{[NO]_{eq}}{[BrNO]_{eq}} + (1-x) \right)^2 \left(\frac{[Br_2]_{eq}}{[BrNO]_{eq}} + \frac{1}{2}(1-x) \right) - 2k_r [BrNO]_{eq} x^2 \quad (22)$$

By letting

$$\alpha = \frac{[NO]_{eq}}{[BrNO]_{eq}} \quad (23)$$

$$K_1 = 2k_f [BrNO]_{eq}^2 \quad (24)$$

$$K_2 = 2k_r [BrNO]_{eq} \quad (25)$$

the differential equation becomes

$$\frac{dx}{dt} = K_1 (\alpha + (1-x))^2 \left(\frac{K_2}{K_1 \alpha^2} + \frac{1}{2}(1-x) \right) - K_2 x \quad (26)$$

The solution to the third-order problem, which was found using Mathematica, is

$$t = \frac{\alpha(f_2 + f_3)}{f_4} \quad (27)$$

where

$$f_1 = \sqrt{-K_2(1+\alpha)^2(K_2(\alpha-1)^2 - 2K_1\alpha^3)}$$

$$f_2 = -2(K_2 - K_2\alpha^2 + K_1\alpha^3) \text{ArcTan}\left(\frac{K_1\alpha^2(x-1+\alpha)+K_2(\alpha^2-1)}{f_1}\right)$$

$$f_3 = f_1 \left(-\ln((x-1)^2) + \ln(K_1\alpha^2(1-x+\alpha)^2 + 2K_2(1+\alpha)(1+x(\alpha-1)+\alpha)) \right)$$

$$f_4 = f_1(K_1\alpha^3 + 4K_2(1 + \alpha))$$

Figure 3 shows a plot of the third-order solution. The values of α , K_1 , and K_2 determine the shape of the curve. All three values must be positive, as defined by equations (23), (24), and (25), but regardless of α , K_1 , and K_2 , the solution has an asymptote at $x=1$.

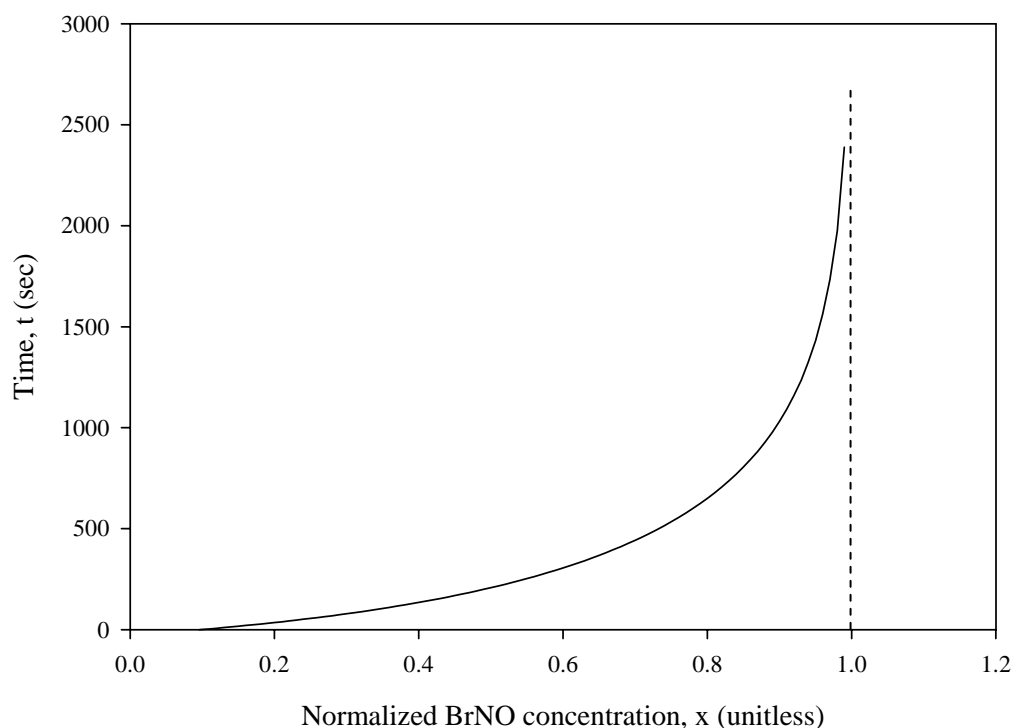


Figure 3. Solution to third-order kinetics problem. Plotted for the case of $P_0(\text{Br}_2) = 0.3$ torr, $P_0(\text{NO}) = 9.7$ torr, $\alpha = 16.15$, $K_1 = 1.13\text{E-}05 \text{ sec}^{-1}$, $K_2 = 8.56\text{E-}05 \text{ sec}^{-1}$.

Values for k_f , k_r , and K_{eq} can be calculated by using the estimated values of α , K_1 and K_2 . Section IV discusses how the solution was fit to the collected spectrometric reaction rate data. However, when this solution is fit to the collected data, the computed values for α , K_1 , and K_2 have error values over 100% larger than the actual value of the parameter. This error results because Tablecurve, the curve fitting program used in this effort, has too many fit parameters to

be certain of the value of any of them. The number of fit parameters in equation (27) can be reduced, consequently reducing the error, by letting

$$K_1 = K_2 * K_{eq} [BrNO]_{eq} \quad (28)$$

and computing α from $[NO]_0$ and $[Br_2]_0$

$$\alpha = \frac{[NO]_{eq}}{[BrNO]_{eq}} = \frac{[NO]_0 - 2n_{eq}}{2n_{eq}} \quad (29)$$

where n_{eq} is a constant determined from K_{eq} , $[NO]_0$ and $[Br_2]_0$ by equation (18).

When an excess of NO is present, the reaction of $Br_2 + 2NO \leftrightarrow 2BrNO$ can be approximated as a first-order reaction, α gets large, $K_1\alpha^2$ becomes much larger than K_2 , and equation (26) reduces to

$$\frac{dx}{dt} = K_1\alpha^2 \left(\frac{1}{2}(1-x) \right) \quad (30)$$

The solution for this equation is

$$x = 1 + C_1 e^{-\frac{1}{2}At} \quad (31)$$

where $A = K_1\alpha^2$. Values for k_f and k_r can be calculated by using the fitted value of A. Section IV discusses how the solution was fit to the data collected in which there was an excess of NO. C_1 is calculated from the initial conditions present in the data.

Appendix A provides the complete calculation for determining the kinetics of the $Br_2 + 2NO \leftrightarrow 2BrNO$ reaction.

III. Experimental Procedure

Experimental Set Up

The experiment was conducted at 10.0 torr total pressure in a 10 cm glass cell with calcium fluoride (CaF_2) windows. A gas handling vacuum system was used to fill the glass cell with a mixture of Br_2 (99.5% pure, Spectrum Chemical Manufacturing) and NO (99% pure, Matheson Gas) at room temperature ($T=293\text{ K}$) with samples containing either an excess of Br_2 or NO. The evacuated glass cell was first backfilled with helium to eliminate any residual chemicals that might be in the cell from previous samples. Additionally, for several samples, the cell was cleaned with methanol to eliminate the buildup of Br_2 on the walls of the cell. A vacuum was pulled on the system until the total pressure was 10 millitorr. After the entire system was evacuated, the glass cell was filled with the substance that had the lower partial pressure. The glass cell was isolated, the vacuum system was again evacuated, and the substance with the higher partial pressure was added to the cell. Each sample had a total pressure of 10.0 torr, but the partial pressures of Br_2 and NO were varied to demonstrate that the initial composition of the mixture did not have an effect on the rate constants.

The first four samples were filled at room temperature with 1.0 torr of NO and 9.0 torr of Br_2 and the remaining samples were filled with 9.0 torr of NO and 1.0 torr of Br_2 , but because of the tendency of bromine to adhere to the internal surfaces of the glass cell and CaF_2 windows, the actual ratio of bromine and NO in the cell at the beginning of data collection is not the same as the original ratio used when mixing the samples. The amount of bromine lost is difficult to quantify because the loss rate depends on the quantity of bromine in the cell and is different each time the cell is filled. The bromine begins to stick to the walls almost immediately making it nearly impossible to prevent this phenomenon. Instead of trying to prevent the loss of Br_2 to the

walls of the cell, the ratio of Br_2 to NO at the start of data collection for each sample was determined from the data collected.

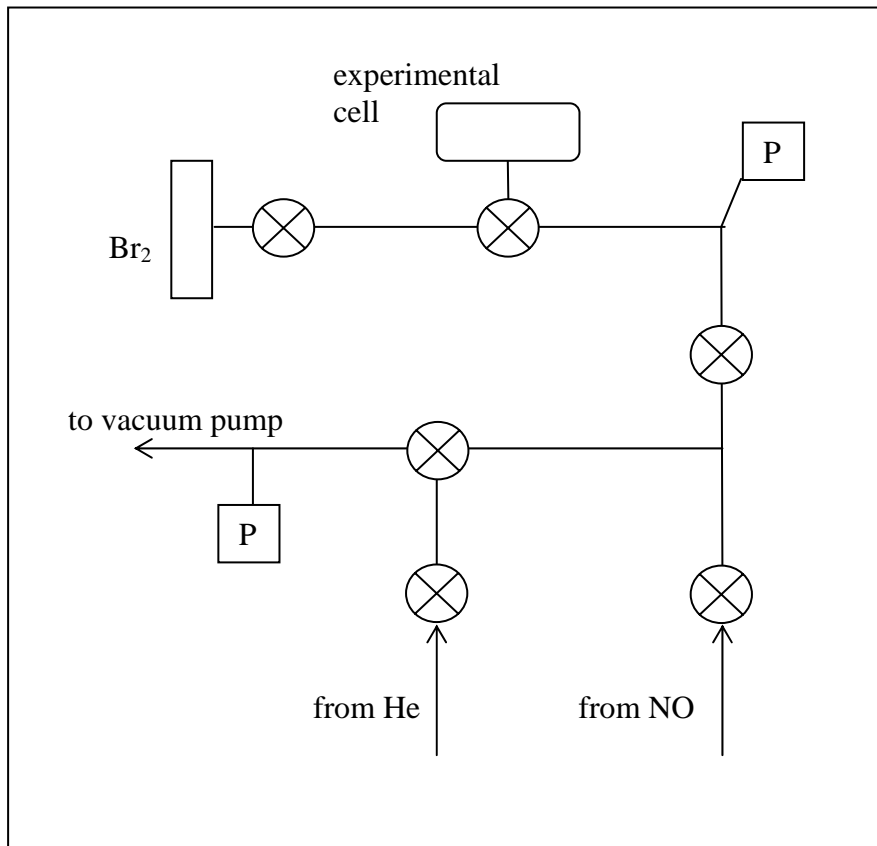


Figure 4. Gas handling vacuum system used to fill the glass cell.

Only one of the previous experiments for determining the forward and reverse rate constants of the $\text{Br}_2 + 2\text{NO} \leftrightarrow 2\text{BrNO}$ reaction addressed the loss of bromine in the sample to the walls. However, no viable solution to the problem was found. The loss of bromine to the walls introduces more error into the determination of the rates, but in this study the error is accounted for by the extrapolation of the pressure ratio of Br_2 to NO at the start of data collection. Section IV explains in more detail how the pressure ratio at the start of data collection is found for each sample.

To demonstrate the tendency of bromine to react with the internal surfaces of the cell, pressure data was recorded with a 100-torr Baratron pressure manometer from two separate samples containing 1.0 torr of bromine in a glass cell over a period of 30 minutes. The first sample measured the pressure drop in both the glass cell and the quarter-inch stainless steel tubing of the gas handling system while the second sample measured the pressure drop in only the tubing. The pressure drop in only the glass cell was found by taking the difference between the two samples because the setup of the gas handling system did not allow for the pressure drop in only the glass cell to be measured directly. This test was performed simply to show that wall effects exist within the sample cells used in this experiment. More data is needed to determine the rate at which the bromine pressure decreases in the cell. The loss of bromine to the internal surfaces of the cell explains why the initial bromine pressure in the cell during data collection is lower than the pressure of bromine originally added to the cell.

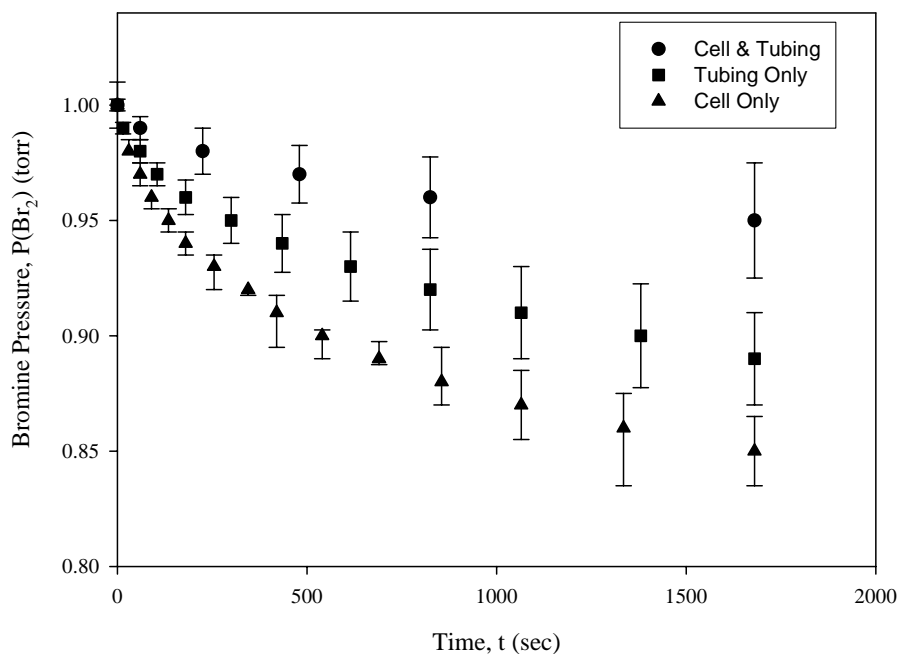


Figure 5. Pressure decrease over time due to loss of Br₂ to the internal surfaces of the system. Samples contained 1.0 torr of Br₂ initially.

Photodissociation and Reformation of BrNO

Immediately after the cell was filled, the mixture of Br₂ and NO began reacting to form BrNO as described in equation (9). The Spectra Physics Millennia VIs J, a CW diode pumped frequency doubled Nd:YVO₄ laser operating at 532 nm, was used to illuminate the cell, causing the photodissociation of BrNO to form Br₂ and NO as shown in equations (7) and (8). The laser output was set to 4 W to maximize beam quality. A neutral density filter wheel was used in conjunction with two cylindrical lenses, which broadened the beam, to decrease the irradiance on the cell to $0.1 \pm 0.05 \text{ mW/cm}^2$ for samples with an excess of NO and $25 \pm 10 \text{ mW/cm}^2$ for samples with an excess of Br₂. The expanded beam was necessary to ensure all the BrNO in the cell was photodissociated. After the mixture had reacted with the light to form only Br₂ and NO, the light was removed from the sample and the mixture was allowed to return to equilibrium.

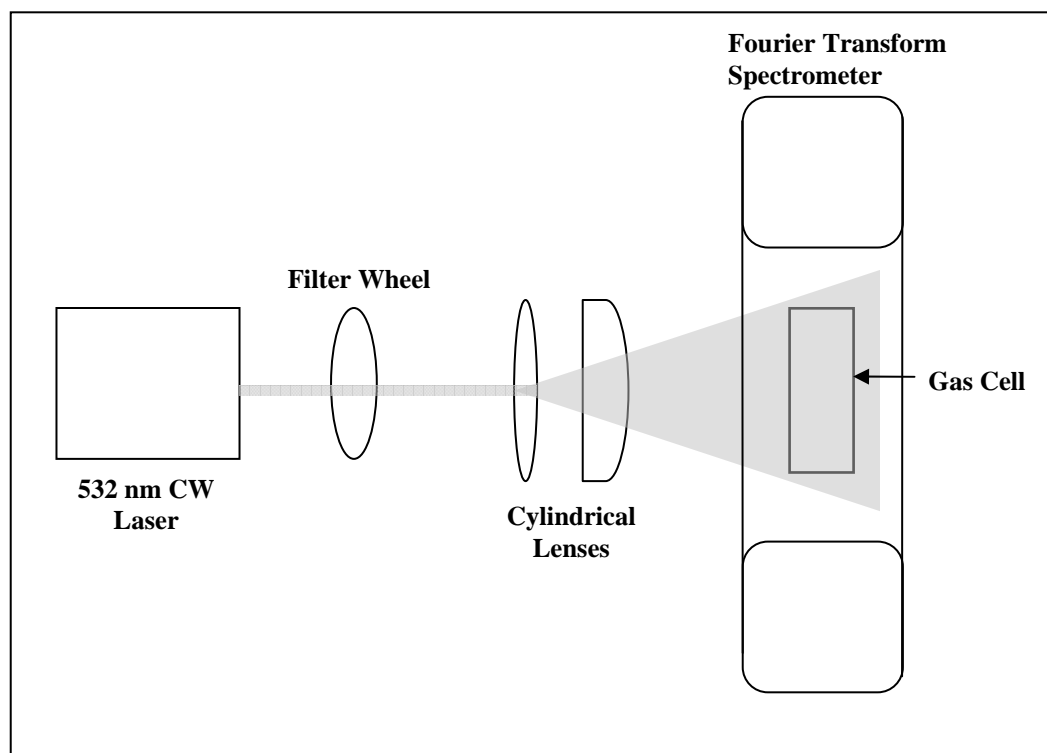


Figure 6. Apparatus used to collect kinetics data.

Collection of Spectra

The spectra used in this experiment were obtained using the Bomem MB 157 FT-IR Spectrometer, which utilizes a modulated broad band IR source and DTGS detector. The infrared beam is modulated before passing through the sample. An interferometer causes each IR frequency to be modulated with a unique frequency of modulation. After the IR beam has passed through the sample, the intensity is detected and the frequencies are demodulated via a Fourier Transform. The absorbance or transmittance spectra are obtained after calculations are executed to combine the pre-recorded reference spectrum and the sample spectrum.

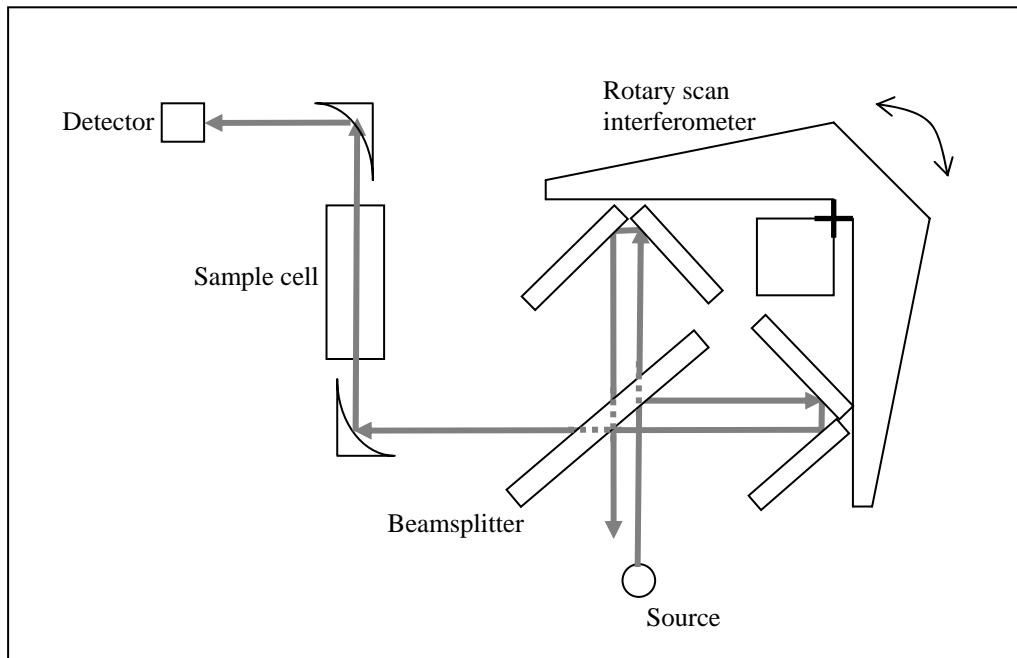


Figure 7. Simplified schematic of the MB 157 FTIR Spectrometer.

The heart of the FTIR spectrometer is the Michelson interferometer. The light from the IR source enters the interferometer and encounters a beamsplitter that reflects one beam towards one cube corner mirror set, which reflects it back towards the beamsplitter, and transmits the other beam towards the other cube corner mirror set, which also reflects it back to the

beamsplitter. As both mirrors move, the optical path length difference between the two beams continuously changes. As a moving mirror is scanned, the two returned beams interfere with different phases, which creates intensity variations. At a given optical path length difference, the interference is constructive at some frequencies and destructive at others. Because the optical path length difference is constantly changing, the various frequencies present in the beam are modulated at different rates.

After leaving the interferometer, the modulated light passes through the sample where some of the IR radiation is absorbed at specific frequencies. The remaining IR radiation reaches the DTGS detector, which converts it to an electrical signal that is then recorded as an interferogram. The spectrum is obtained from the interferogram using a Fourier Transform.²

Safety Precautions

The primary hazards associated with this experiment were the laser and the reactants used (Br_2 and NO). A Class IV laser was operated at 4 W to illuminate the sample of BrNO during this experiment. Permanent eye damage can result from unprotected exposure to laser radiation. Appropriate laser safety glasses were worn and all jewelry was removed during the use of the laser. Additionally, bromine and nitric oxide are serious health hazards. Bromine, a dark red liquid at room temperature, volatilizes rapidly to form a red vapor with a strong, disagreeable odor. The vapor is very irritating to the eyes and throat; the liquid causes painful sores when spilled on the skin. Nitric oxide is a colorless, poisonous gas that reacts rapidly with oxygen to form NO_2 , a mildly poisonous brown vapor that is one of the principle components of smog.¹⁷ NO gas detectors monitored for leaks around the area containing the gas handling system. Great care was taken during this experiment to avoid direct exposure to any of these chemicals.

IV. Results

Third-Order Solution

A 2 cm^{-1} resolution FTIR transmittance spectrum was collected approximately every six seconds for every sample cell from the moment the laser was turned on and began reacting with the sample until the sample reached equilibrium after the laser was removed. The spectra collected while the laser was illuminating the sample were used to verify that all the BrNO had been dissociated into Br₂ and NO. The spectra collected after the laser was turned off were used to determine the forward and reverse reaction rate constants for $\text{Br}_2 + 2\text{NO} \xrightleftharpoons[k_r]{k_f} 2\text{BrNO}$.

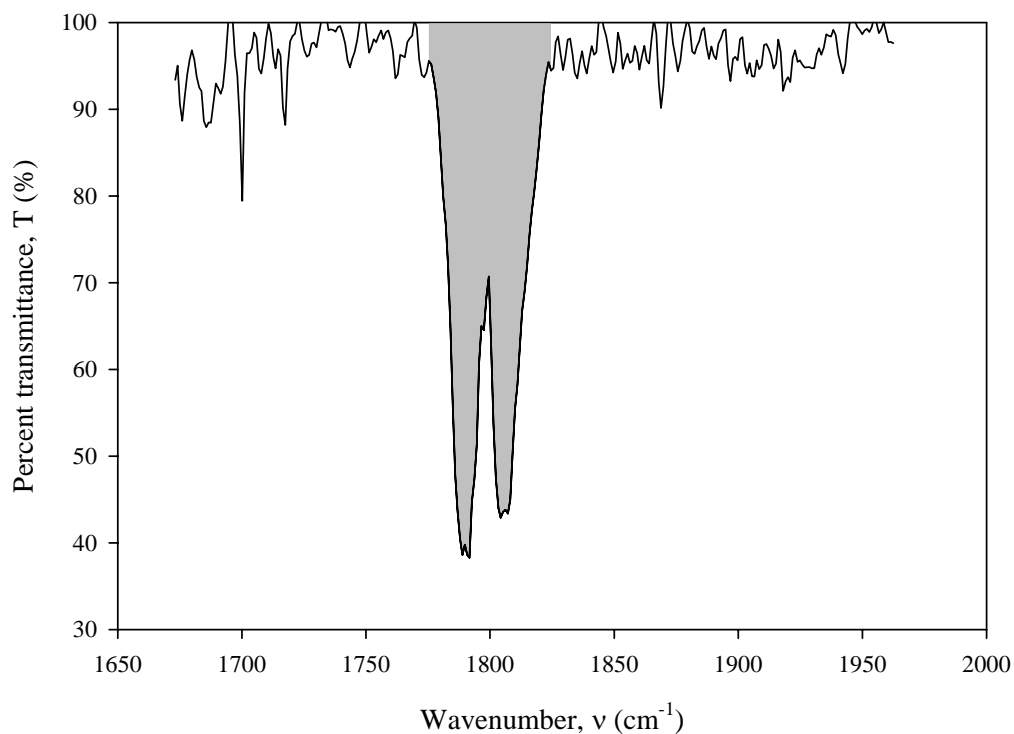


Figure 8. Example of area measured “under” the BrNO $\nu=1$ line by Bomem GRAMS/32. $P_{\text{eq}}(\text{BrNO}) = 0.565$ torr

At equilibrium, a very strong $\nu=1$ line of BrNO is observed in the FTIR spectra collected. Using Bomem GRAMS/32, the area under the BrNO line could be calculated for all the spectra acquired from each sample. These areas were normalized with the area under the peak when the sample was at equilibrium. As explained in Section II the normalized value of the area under the BrNO peak is equal to the normalized concentration of BrNO, x , which is needed to fit the data to the third-order solution of the reaction. However, the solution in equation (27) for the third-order kinetics problem cannot be solved for x in terms of t , but instead the data points must be reversed to allow equation (27) to be fit to the data. The error values of the normalized BrNO concentration for each of the samples were estimated using the standard deviation of the area measurements.

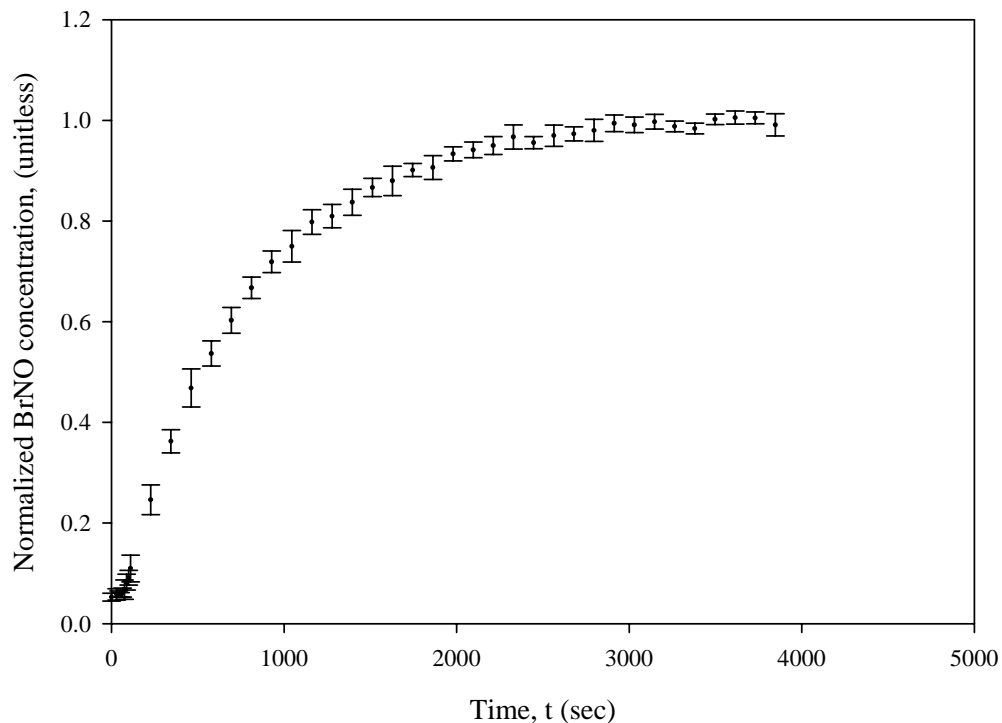


Figure 9. Example of normalized BrNO concentration, x , as a function of time, t . The laser is turned off at time=0 sec and the sample is allowed to reach equilibrium. $P_0(\text{Br}_2) = 0.3$ torr, $P_0(\text{NO}) = 9.7$ torr

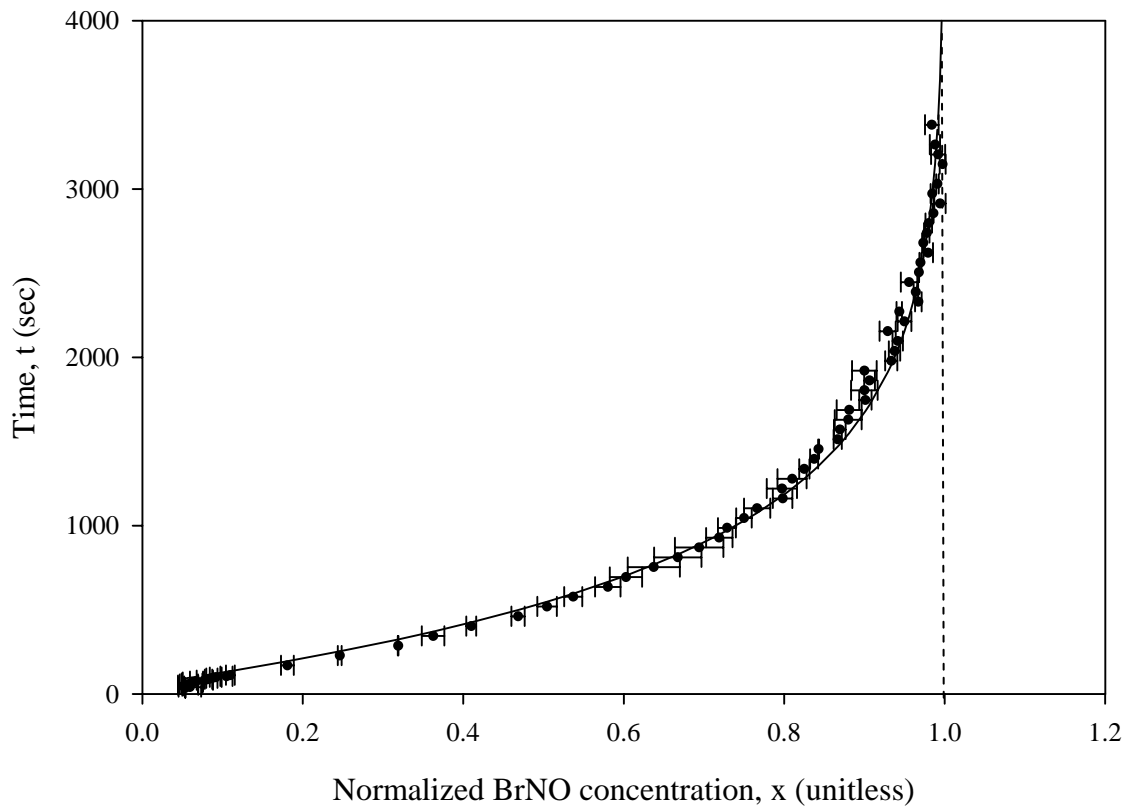


Figure 10. Example of third-order solution fit ($r^2 = 0.952$) to observed data with K_2 as the only fit parameter. $P_0(\text{Br}_2) = 0.28$ torr, $P_0(\text{NO}) = 9.72$ torr

Using Tablecurve, a curve fitting program, a value for K_2 was found for each of the samples. The value for K_2 is dependent on the value of α , which in turn is dependent on $[\text{Br}_2]_0$ and $[\text{NO}]_0$ according to equation (29). The values for $[\text{Br}_2]_0$ and $[\text{NO}]_0$ needed to be established from the data collected because of the loss of Br_2 to the walls of the cell. Using a trial and error method, the total pressure in the cell was held constant at 10.0 torr, while the initial fraction of NO ($f(\text{NO})_0$) and the initial fraction of Br_2 ($f(\text{Br}_2)_0$) were varied. The values used for $[\text{Br}_2]_0$ and $[\text{NO}]_0$ were the values which gave the best curve fit to the data when calculating K_2 .

Table 2. Example of calculation of $[\text{Br}_2]_0$ and $[\text{NO}]_0$ from the curve fit data.
 $P^T = 10.0$ torr, $T=293$ K, $K_{\text{eq}} = 6.71\text{E-}18$ $\text{cm}^3/\text{molecule}$

$f(\text{NO})_0$ (unitless)	$f(\text{Br}_2)_0$ (unitless)	$\alpha = \frac{[\text{NO}]_{\text{eq}}}{[\text{BrNO}]_{\text{eq}}}$ (unitless)	$K_{\text{eq}}[\text{BrNO}]_{\text{eq}}$ (unitless)	K_1 (sec^{-1})	K_2 (sec^{-1})	K_2 Error (sec^{-1})	r^2
0.900	0.100	4.67	0.351	--	won't fit	--	--
0.910	0.090	5.21	0.324	--	won't fit	--	--
0.920	0.080	5.88	0.296	--	won't fit	--	--
0.930	0.070	6.74	0.266	--	won't fit	--	--
0.940	0.060	7.91	0.233	--	won't fit	--	--
0.950	0.050	9.55	0.199	2.18E-05	1.10E-04	5.33E-06	0.744
0.960	0.040	12.02	0.163	1.49E-05	9.13E-05	2.82E-06	0.886
0.965	0.035	13.79	0.144	1.20E-05	8.32E-05	2.00E-06	0.928
0.970	0.030	16.16	0.125	9.44E-06	7.55E-05	1.50E-06	0.949
0.972	0.028	17.34	0.117	8.48E-06	7.24E-05	1.39E-06	0.952
0.975	0.025	19.48	0.105	7.12E-06	6.77E-05	1.32E-06	0.950
0.977	0.023	21.22	0.097	6.26E-06	6.44E-05	1.32E-06	0.945
0.980	0.020	24.46	0.085	5.05E-06	5.93E-05	1.36E-06	0.930
0.990	0.010	49.43	0.043	1.67E-06	3.84E-05	1.38E-06	0.826

Table 3. Summary of partial pressures at the start of data collection. Values extrapolated from the measured FTIR data.

Sample	Total Pressure (torr)	$P(\text{NO})_0$ (torr)	$P(\text{Br}_2)_0$ (torr)
1	10.0	0.93	9.07
2	10.0	0.92	9.08
3	10.0	0.92	9.08
4	10.0	0.92	9.08
5	10.0	9.75	0.25
6	10.0	9.70	0.30
7	10.0	9.75	0.25
8	10.0	9.77	0.23
9	10.0	9.75	0.25
10	10.0	9.70	0.30
11	10.0	9.70	0.30
12	10.0	9.75	0.25
13	10.0	9.65	0.35
14	10.0	9.65	0.35
15	10.0	9.65	0.35

After determining the pressure values of Br₂ and NO at the start of data collection for each sample, the values of k_f and k_r were calculated using the initial concentrations of Br₂ and NO, which are easily calculated from the initial pressures using the ideal gas law, the equilibrium constant, and the value of K₂ found by fitting the third-order solution to the data. The mean value $\pm 1\sigma$, calculated from the data in Table 4, of k_f is $1.55 \pm 0.19 \times 10^{-38} \text{ cm}^6/\text{molecule}^2\text{-s}$ and of k_r is $2.31 \pm 0.28 \times 10^{-21} \text{ cm}^3/\text{molecule-s}$.

Table 4. Calculated k_f and k_r values using data fit to third-order solution with K₂ as only fit parameter.

P ₀ (Br ₂) (torr)	P ₀ (NO) (torr)	k _f (10 ⁻³⁸ cm ⁶ /molecule ² -s)	k _r (10 ⁻²¹ cm ³ /molecule-s)
9.07	0.93	1.395	2.079
9.08	0.92	1.398	2.084
9.08	0.92	1.342	2.000
9.08	0.92	1.236	1.843
0.25	9.75	1.411	2.104
0.30	9.70	1.472	2.194
0.25	9.75	1.605	2.393
0.23	9.77	1.617	2.411
0.28	9.72	1.391	2.074
0.30	9.70	1.595	2.377
0.30	9.70	1.604	2.391
0.25	9.75	1.735	2.586
0.35	9.65	1.693	2.523
0.35	9.65	1.885	2.810
0.35	9.65	1.836	2.736

The values calculated for k_f and k_r using the third-order solution with only K₂ as a fit parameter are refined by fitting both K₁ and K₂ to the third-order solution with a fixed value for α . Keeping α fixed holds the error in the computed values of K₁ and K₂ to less than 10% of the value. However, any attempt to fit all three variables, α , K₁, and K₂, to the collected kinetics data, gives error values of greater than 100% for all of the fit parameters, causing the fit parameters to be essentially useless. Therefore, the fit of K₁ and K₂ to the kinetics data gives the

most reliable values for k_f and k_r . Additionally, the value of K_{eq} can be calculated from the values determined for k_f and k_r . The values of the rate constants and the equilibrium constant determined in this experiment are listed in Table 6 along with the results from previous efforts. The data used to determine k_f , k_r , and K_{eq} is shown in Table 5.

Table 5. Calculated K_{eq} , k_f and k_r values using data fit to third-order solution with K_1 and K_2 as fit parameters.

$P_0(\text{Br}_2)$ (torr)	$P_0(\text{NO})$ (torr)	k_f ($10^{-38} \text{ cm}^6/\text{molecule}^2\text{-s}$)	k_r ($10^{-21} \text{ cm}^3/\text{molecule-s}$)	K_{eq} (atm^{-1})
9.07	0.93	1.483	2.217	168
9.08	0.92	1.372	2.044	168
9.08	0.92	1.326	1.976	168
9.08	0.92	1.184	1.763	168
0.25	9.75	1.394	2.152	162
0.30	9.70	1.542	2.011	192
0.25	9.75	1.614	2.361	171
0.23	9.77	1.628	2.372	172
0.28	9.72	1.409	2.023	174
0.30	9.70	1.628	2.298	177
0.30	9.70	1.724	2.151	201
0.25	9.75	1.647	2.826	146
0.35	9.65	1.664	2.618	159
0.35	9.65	1.867	2.865	163
0.35	9.65	1.861	2.642	176

Table 6. Values of k_f , k_r , and K_{eq} obtained in this and previous efforts. The quantities listed for this study are the means $\pm 1\sigma$ determined from the data in Table 5.

	$k_f (10^{-38} \text{ cm}^6/\text{molecule}^2\text{-s})$	$k_r (10^{-21} \text{ cm}^3/\text{molecule-s})$	$K_{eq} (\text{atm}^{-1})$	T (K)
This Effort	1.56 ± 0.20	2.29 ± 0.33	171 ± 13	293 ± 1
Godfrey ⁴	1.40 ± 0.18	2.09 ± 0.55	168 ± 23	293 ± 1
Hippler ⁷	1.68 ± 0.11	--	--	298
Houel ¹⁰	1.60 ± 0.16	2.67	150 ± 48	303 ± 0.5
Hisatsune ⁸	1.32 ± 0.14	3.71	89	303

First-Order Solution

The forward and reverse reaction rate constants could also be calculated using the first-order solution, equation (31), for samples that contained an excess of NO. The parameters A, which equals $K_1\alpha^2$, and C_1 were fit to the data. Mathematically, at the point $x=0$, $t=0$, C_1 is equal to -1. In this experiment, the data determined that C_1 was approximately -1, showing that the data was very close to what was expected. Due to system noise, the concentration of BrNO is never actually measured as zero, even after all the BrNO has reacted to form NO and Br₂.

The variable α was calculated using the values of $[\text{Br}_2]_0$ and $[\text{NO}]_0$ determined while fitting the third-order solution to the data. k_f was then calculated from the fit parameter A and k_r was found using k_f and the equilibrium constant. The mean value $\pm 1\sigma$, calculated from the data in Table 7 of k_f is $1.91 \pm 0.69 \times 10^{-38} \text{ cm}^6/\text{molecule}^2\text{-s}$ and of k_r is $2.84 \pm 1.03 \times 10^{-21} \text{ cm}^3/\text{molecule-s}$.

Table 7. Calculated k_f and k_r values using data fit to first-order solution with $A=K_1\alpha^2$ and C_1 as fit parameters.

$P_0(\text{Br}_2)$ (torr)	$P_0(\text{NO})$ (torr)	$k_f(10^{-38} \text{ cm}^6/\text{molecule}^2\text{-s})$	$k_r(10^{-21} \text{ cm}^3/\text{molecule-s})$
0.25	9.75	1.42E-38	2.12E-21
0.30	9.70	1.62E-38	2.42E-21
0.25	9.75	1.42E-38	2.11E-21
0.23	9.77	1.30E-38	1.94E-21
0.25	9.75	1.43E-38	2.13E-21
0.30	9.70	1.67E-38	2.49E-21
0.30	9.70	1.63E-38	2.43E-21
0.25	9.75	1.60E-38	2.39E-21
0.35	9.65	3.00E-38	4.48E-21
0.35	9.65	2.92E-38	4.36E-21
0.35	9.65	2.96E-38	4.42E-21

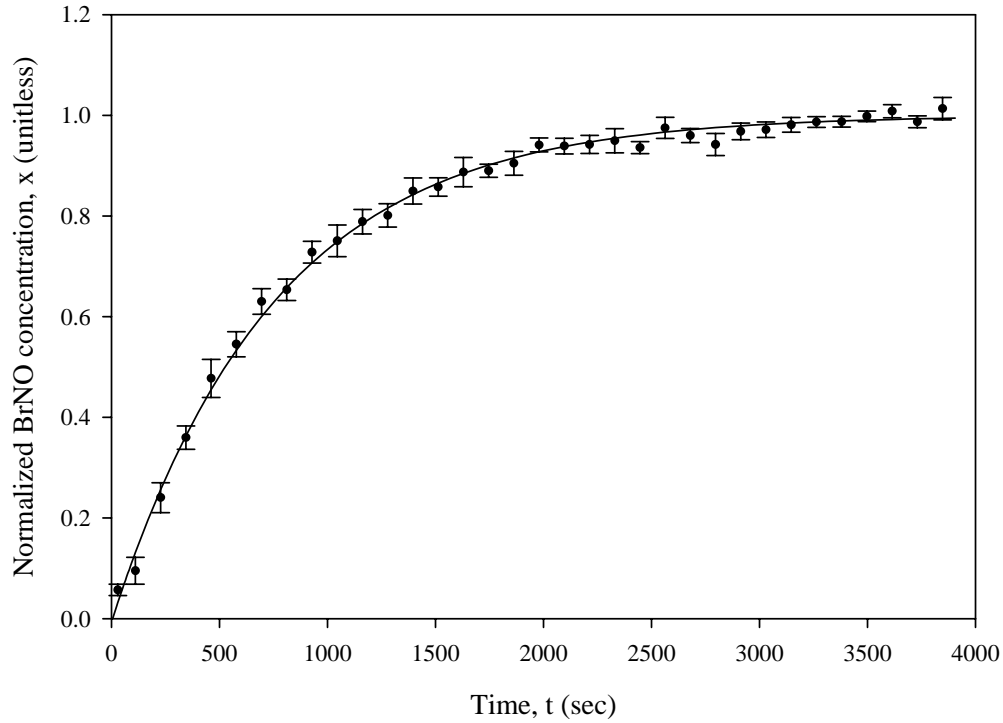


Figure 11. Example of first-order solution fit ($r^2 = 0.997$) to observed data with $A=K_1\alpha^2$ and C_1 as fit parameters. $P_0(\text{Br}_2) = 0.25$ torr, $P_0(\text{NO}) = 9.75$ torr

Solution Near Zero BrNO Concentration

The original differential equation, equation (26), becomes equation (32) as x approaches zero.

$$\left. \frac{dx}{dt} \right|_{x=0} = K_1(\alpha + 1)^2 \left(\frac{K_2}{K_1\alpha^2} + \frac{1}{2} \right) \quad (32)$$

Table 8 illustrates the difference between the theoretical slope calculated with this equation and the slope measured from the data. The slope of each sample was measured near $x=0$ by computing the linear regression of the first 50 data samples, which occurs when time is less than 286 seconds.

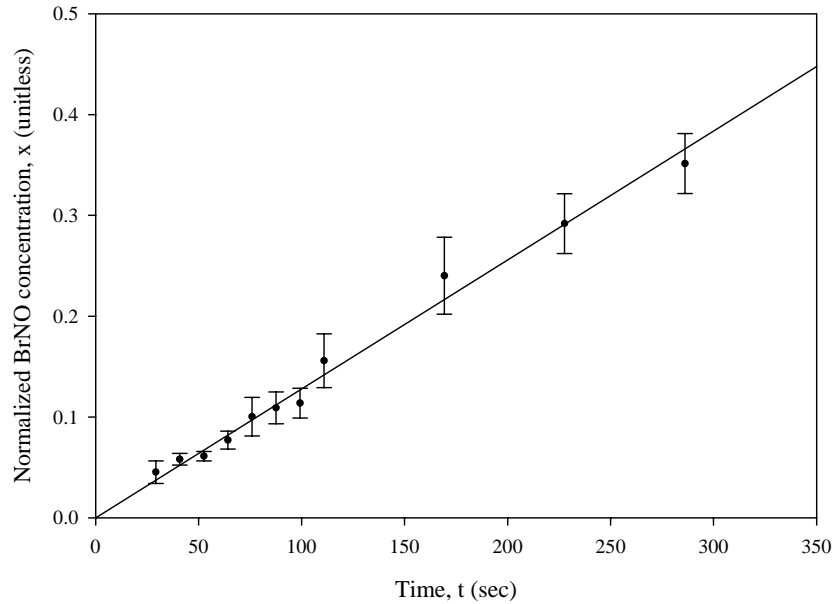


Figure 12. Example of concentration versus time near $[\text{BrNO}]_t$ equals zero. $P_0(\text{Br}_2) = 0.30$ torr, $P_0(\text{NO}) = 9.70$ torr. Measured slope near concentration equals zero is 0.0013 sec^{-1} . Calculated slope equals 0.0015 sec^{-1} .

Table 8. Measured versus calculated slope near $[\text{BrNO}]_t = 0$

Sample	α (unitless)	K_1 (sec^{-1})	K_2 (sec^{-1})	$\left. \frac{dx}{dt} \right _{x=0}^{\text{measured}}$ (sec^{-1})	$\left. \frac{dx}{dt} \right _{x=0}^{\text{theoretical}}$ (sec^{-1})
1	0.72	9.37E-06	7.87E-05	0.00039	0.00047
2	0.72	8.55E-06	7.22E-05	0.00028	0.00043
3	0.72	8.30E-06	6.99E-05	0.00033	0.00041
4	0.72	7.37E-06	6.23E-05	0.00032	0.00037
5	19.48	7.11E-06	6.75E-05	0.00112	0.00156
6	16.16	9.36E-06	7.49E-05	0.00128	0.00146
7	19.48	7.80E-06	7.41E-05	0.00111	0.00172
8	21.21	6.68E-06	6.88E-05	0.00093	0.00172
9	19.48	7.85E-06	7.46E-05	0.00117	0.00173
10	16.16	1.07E-05	8.56E-05	0.00125	0.00167
11	16.16	1.00E-05	8.01E-05	0.00133	0.00156
12	19.48	7.85E-06	7.46E-05	0.00121	0.00173
13	13.79	1.62E-05	1.13E-04	0.00228	0.00190
14	13.79	1.78E-05	1.23E-04	0.00218	0.00208
15	13.79	1.64E-05	1.14E-04	0.00223	0.00192

Ideally the theoretical slope would equal the measured slope, but due to errors in calculating both the measured and theoretical slopes, the values are slightly different. Error is introduced into the calculation of the measured slope from the choice of endpoints and the variability of the measured data. Due to noise in system, the normalized concentration is never measured as zero, which causes most of the error in the measured slope. The calculated theoretical slope contains the statistical error in K_1 and K_2 .

Error

Error in the rates is mostly due to the uncertainty in the initial pressure measurements. The error in the pressure of Br_2 and NO added to the cell is ± 0.01 torr, due to the limitations of the manometer used to monitor the pressure. The error in the pressures of Br_2 and NO at the start of data collection is larger, however, because the values had to be extrapolated from the collected kinetics data due to the loss of Br_2 to the walls of the cell. The error in determining the initial values of Br_2 and NO is ± 0.1 torr.

Temperature variations also change the pressure in the cell. The temperature inside the cell was not measured, but the relatively low heat capacity of the gas mixture permits the assumption of thermal equilibrium inside the cell. The heat capacity of the glass cell also allows the assumption that sudden temperature variations within the cell did not occur. Regardless, a ± 1 K temperature variation at 293 K changes the pressure of a 10 torr ideal gas by ± 0.034 torr, which is small when compared to the ± 0.1 torr error in the extrapolated initial pressure values.

The statistical error in fitting the parameters, K_2 and K_1 , to the measured data was another source of error. The amount of error in the fit parameters to the third-order solution was small compared to the actual value of the parameter, at less than 10% of the value, whereas the error in the fit parameters to the first-order solution was on average over 20% of the value. Additionally, Tablecurve calculated how well the theoretical solution, containing the computed values of K_2

and K_1 , fit to the measured data using both the Linear Least Squares Method and the Levenberg-Marquardt (nonlinear least squares) Method. For every sample an r^2 value was calculated using both methods, where $r^2 = 1$ indicates that the equation fits the data perfectly. In this experiment both methods gave identical r^2 values to two significant figures. For the third-order solution the average r^2 value over all the samples was $r^2 = 0.941$. For the first-order solution, the theoretical solution fit the measured data nearly perfectly with an average r^2 value of 0.998.

V. Conclusions

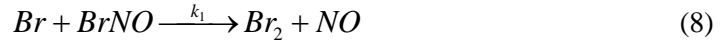
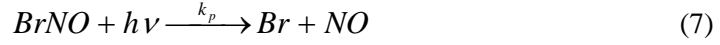
The agreement between the measured reaction rate data and the theoretical solution by the fitting technique provides further evidence that the reaction of Br₂ and NO to form BrNO is effectively described by third-order kinetics. Fitting both K₁, which is directly related to k_f, and K₂, which is directly related to k_r, to the third-order solution produced the most reliable values for k_f and k_r. As shown in Table 6 of Section IV, the value of k_f found in this effort is approximately equal to previously determined values. In this effort $k_f = 1.56 \pm 0.20 \times 10^{-38} \text{ cm}^6/\text{molecule}^2\text{-s}$ and in previous efforts k_f ranged from 1.18 to 1.79 x 10⁻³⁸ cm⁶/molecule²-s, when including the error bounds. The values of k_r and K_{eq} determined in this effort are nearly equal to the values found by Godfrey, but are not equivalent to other previously determined values. In this effort $k_r = 2.29 \pm 0.33 \times 10^{-21} \text{ cm}^3/\text{molecule-s}$, which is very close to Godfrey's value of $2.09 \pm 0.55 \times 10^{-21} \text{ cm}^3/\text{molecule-s}$, but differs from earlier values of 2.67 and 3.71 x 10⁻²¹ cm³/molecule-s. The method used to solve the third-order kinetics problem in this effort is similar to Godfrey's technique, which may partially explain the close proximity of the values. Additionally, only Godfrey's and this research accounted for the loss of Br₂ to the cell walls. The reaction rate constant was determined more accurately by accounting for this loss.

The reaction rates determined in this experiment can be used in the design of the tunable laser which utilizes the NO transition at 5.4 microns. The reaction rates tell how much BrNO is present at equilibrium and can be used to determine how much the BrNO absorption band at 5.6 microns (v=1) will interfere with the desired NO transition.

Appendix A. Detailed Calculation of the Kinetics Equations

Third-order solution

The reactions of interest are:



The rate of change of the concentration of BrNO over time is described by

$$\frac{d[BrNO]_t}{dt} = -k_p [BrNO]_t I_p - k_1 [Br]_t [BrNO]_t + 2k_f [NO]_t^2 [Br_2]_t - 2k_r [BrNO]_t^2 \quad (10)$$

When the laser is shut off ($I_p = 0$), the first two terms go away and equation (10) becomes

$$\frac{d[BrNO]_t}{dt} = 2k_f [NO]_t^2 [Br_2]_t - 2k_r [BrNO]_t^2 \quad (11)$$

By defining the normalized concentration of BrNO as

$$x = \frac{[BrNO]_t}{[BrNO]_{eq}} \quad (12)$$

where the max value of $x = 1$, and solving for $[BrNO]_t$, gives

$$[BrNO]_t = x [BrNO]_{eq} \quad (19)$$

Additionally,

$$[NO]_t = [NO]_{eq} + [BrNO]_{eq} - [BrNO]_t$$

$$\Rightarrow [NO]_t = [NO]_{eq} + [BrNO]_{eq}(1-x) \quad (20)$$

$$2[Br_2]_t = 2[Br_2]_{eq} + [BrNO]_{eq} - [BrNO]$$

$$\Rightarrow [Br_2]_t = [Br_2]_{eq} + \frac{1}{2}[BrNO]_{eq}(1-x) \quad (21)$$

Substituting, equations (19), (20) and (21) into equation (11) the rate of change of the concentration of BrNO over time becomes

$$\frac{d[BrNO]_t}{dt} = 2k_f([NO]_{eq} + [BrNO]_{eq}(1-x))^2 \left([Br_2]_{eq} + \frac{1}{2}[BrNO]_{eq}(1-x) \right) - 2k_r[BrNO]_{eq}^2 x^2 \quad (32)$$

Using the chain rule, the change in x over time is

$$\frac{dx}{dt} = \frac{d[BrNO]_t}{dt} * \frac{1}{[BrNO]_{eq}} \quad (33)$$

or

$$\frac{dx}{dt} = 2k_f [BrNO]_{eq}^2 \left(\frac{[NO]_{eq}}{[BrNO]_{eq}} + (1-x) \right)^2 \left(\frac{[Br_2]_{eq}}{[BrNO]_{eq}} + \frac{1}{2}(1-x) \right) - 2k_r [BrNO]_{eq} x^2 \quad (22)$$

By letting

$$\alpha = \frac{[NO]_{eq}}{[BrNO]_{eq}} \quad (23)$$

$$K_1 = 2k_f [BrNO]_{eq}^2 \quad (24)$$

$$K_2 = 2k_r [BrNO]_{eq} \quad (25)$$

equation (22) becomes

$$\frac{dx}{dt} = K_1(\alpha + (1-x))^2 \left(\frac{[Br_2]_{eq}}{[BrNO]_{eq}} + \frac{1}{2}(1-x) \right) - K_2x^2 \quad (34)$$

$[Br_2]_{eq}/[BrNO]_{eq}$ can be found in terms of α , K_1 , and K_2 using the equilibrium constant.

$$K_{eq} = \frac{k_f}{k_r} = \frac{[BrNO]_{eq}^2}{[NO]_{eq}^2 [Br_2]_{eq}} \quad (17)$$

$$\frac{[Br_2]_{eq}}{[BrNO]_{eq}} = \frac{k_r}{k_f} \frac{[BrNO]_{eq}}{[NO]_{eq}^2} = \frac{K_0}{\alpha^2} \quad (35)$$

$$K_0 = \frac{k_r}{k_f} \frac{K_2}{K_1} \quad (36)$$

Inserting equations (35) and (36) into equation (34) gives

$$\frac{dx}{dt} = K_1(\alpha + (1-x))^2 \left(\frac{K_2}{K_1\alpha^2} + \frac{1}{2}(1-x) \right) - K_2x^2 \quad (26)$$

The solution for the third-order problem is found by separating the variables and integrating both sides.

$$\int dt = \int \frac{dx}{K_1(\alpha + (1-x))^2 \left(\frac{K_2}{K_1\alpha^2} + \frac{1}{2}(1-x) \right) - K_2x^2} \quad (37)$$

From Mathematica, the solution is

$$t = \frac{\alpha(f_2 + f_3)}{f_4} \quad (27)$$

where

$$f_1 = \sqrt{-K_2(1+\alpha)^2(K_2(\alpha-1)^2 - 2K_1\alpha^3)}$$

$$f_2 = -2(K_2 - K_2\alpha^2 + K_1\alpha^3) \text{ArcTan}\left(\frac{K_1\alpha^2(x-1+\alpha)+K_2(\alpha^2-1)}{f_1}\right)$$

$$f_3 = f_1\left(-\ln((x-1)^2) + \ln(K_1\alpha^2(1-x+\alpha)^2 + 2K_2(1+\alpha)(1+x(\alpha-1)+\alpha))\right)$$

$$f_4 = f_1(K_1\alpha^3 + 4K_2(1+\alpha))$$

The number of fit parameters in the solution can be reduced by solving K_1 in terms of K_2 .

$$K_1 = 2k_f [BrNO]_{eq}^2 \quad (24)$$

$$K_2 = 2k_r [BrNO]_{eq} \quad (25)$$

$$[BrNO]_{eq} = \frac{K_2}{2k_r} \quad (38)$$

$$K_1 = \frac{K_2}{2k_r} * 2k_f [BrNO]_{eq} = K_2 * K_{eq} [BrNO]_{eq} \quad (39)$$

Using the relationship in equation (40), the third-order solution becomes

$$t = \frac{\alpha(f_2' + f_3')}{f_4'} \quad (40)$$

where

$$f_1' = \sqrt{-K_2(1+\alpha)^2(K_2(\alpha-1)^2 - 2(K_2 * K_{eq} [BrNO]_{eq})\alpha^3)}$$

$$f_2' = -2(K_2 - K_2\alpha^2 + (K_2 * K_{eq} [BrNO]_{eq})\alpha^3) \text{ArcTan}\left(\frac{(K_2 * K_{eq} [BrNO]_{eq})\alpha^2(x-1+\alpha)+K_2(\alpha^2-1)}{f_1'}$$

$$f_3' = f_1'\left(-\ln((x-1)^2) + \ln((K_2 * K_{eq} [BrNO]_{eq})\alpha^2(1-x+\alpha)^2 + 2K_2(1+\alpha)(1+x(\alpha-1)+\alpha))\right)$$

$$f_4' = f_1'((K_2 * K_{eq} [BrNO]_{eq})\alpha^3 + 4K_2(1+\alpha))$$

First-order solution

When there is an excess of NO, the $\text{Br}_2 + 2\text{NO} \leftrightarrow 2\text{BrNO}$ follows pseudo first-order kinetics and equation (26) is simplified because α becomes very large and $K_1\alpha^2$ becomes much larger than K_2 under these conditions.

$$\frac{dx}{dt} = K_1(\alpha + (1-x))^2 \left(\frac{K_2}{K_1\alpha^2} + \frac{1}{2}(1-x) \right) - K_2x^2 \quad (26)$$

$$\alpha \rightarrow \infty$$

$$K_1\alpha^2 \gg K_2$$

$$K_1\alpha^2 = 2k_f [\text{BrNO}]_{eq}^2 \frac{[\text{NO}]_{eq}^2}{[\text{BrNO}]_{eq}^2} = 2k_f [\text{NO}]_{eq}^2 \quad (41)$$

Using an intermediate step, the change in x over time becomes

$$\frac{dx}{dt} = K_1\alpha^2 \left(\frac{1}{2}(1-x) \right) - K_2x^2 = K_1\alpha^2 \left[\left(\frac{1}{2}(1-x) \right) - \frac{K_2}{K_1\alpha^2}x^2 \right]$$

$$\frac{dx}{dt} = K_1\alpha^2 \left(\frac{1}{2}(1-x) \right) \quad (30)$$

Solving the differential equation gives

$$x = 1 + C_1 e^{-\frac{1}{2}At} \quad (31)$$

where $A = K_1\alpha^2$ and $C_1 = -1$ at $x(0)=0$.

Appendix B. Kinetics Data Obtained from FTIR spectra

The following figures show the kinetics data collected from the FTIR spectra for each sample. The normalized concentration, x , was plotted as a function of time, t . The normalized concentration of BrNO was found by dividing the area under the BrNO $\nu=1$ line at time= t by the area under the BrNO $\nu=1$ line at equilibrium. For each sample the laser was turned off at time= 0 sec and the sample was allowed to reach equilibrium.

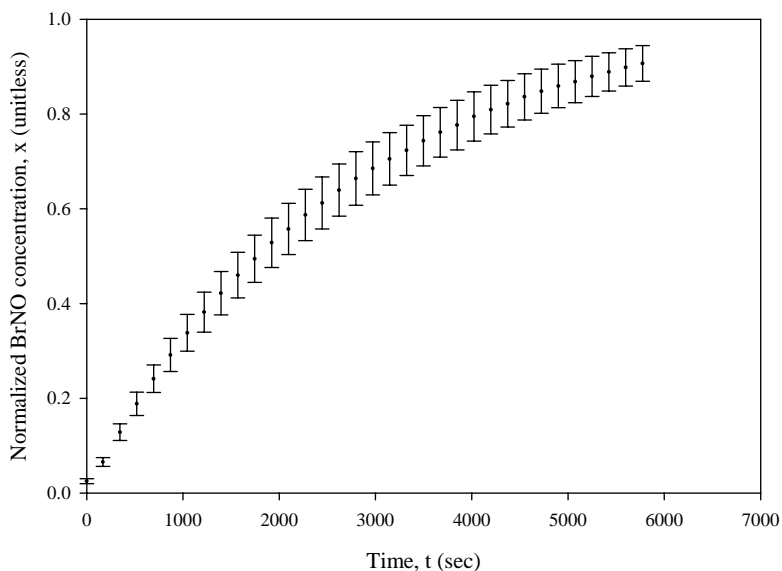


Figure 13. Normalized BrNO concentration, x , plotted as a function of time, t , for sample 1. $P_0(\text{Br}_2) = 9.07$ torr, $P_0(\text{NO}) = 0.93$ torr

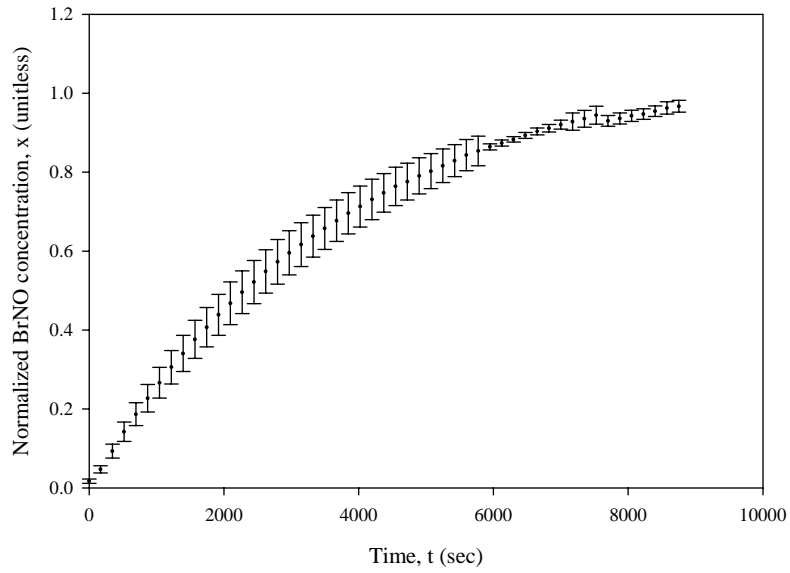


Figure 14. Normalized BrNO concentration, x , plotted as a function of time, t , for sample 2. $P_0(\text{Br}_2) = 9.08$ torr, $P_0(\text{NO}) = 0.92$ torr

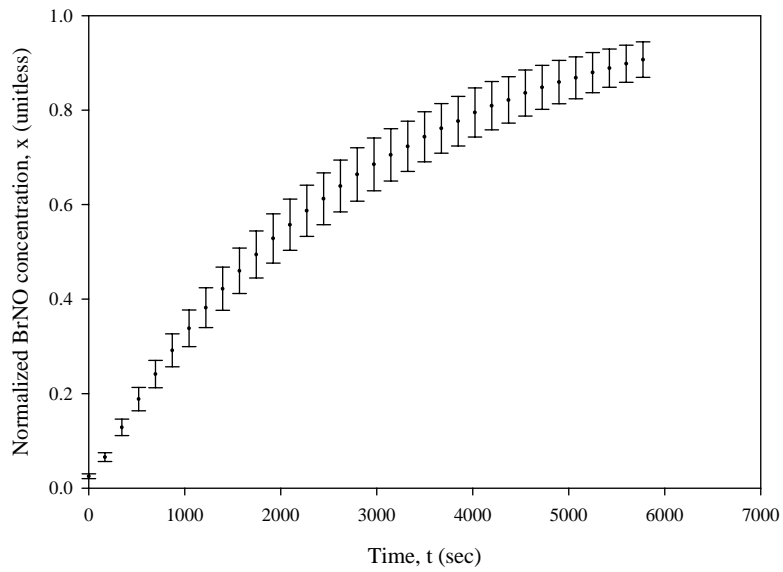


Figure 15. Normalized BrNO concentration, x , plotted as a function of time, t , for sample 3. $P_0(\text{Br}_2) = 9.08$ torr, $P_0(\text{NO}) = 0.92$ torr

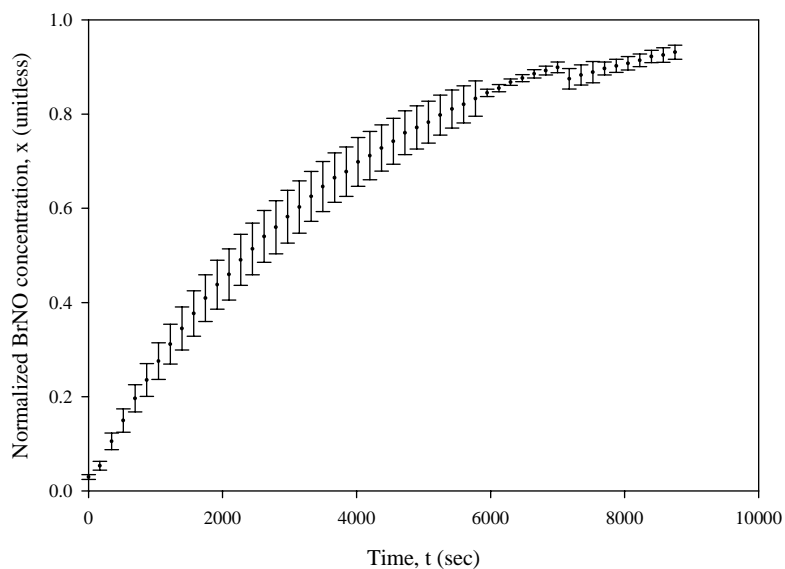


Figure 16. Normalized BrNO concentration, x , plotted as a function of time, t , for sample 4. $P_0(\text{Br}_2) = 9.08$ torr, $P_0(\text{NO}) = 0.92$ torr

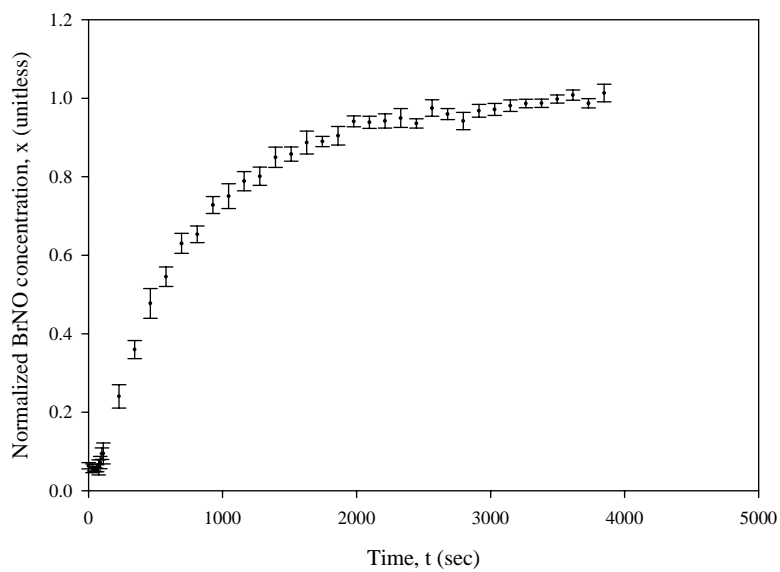


Figure 17. Normalized BrNO concentration, x , plotted as a function of time, t , for sample 5. $P_0(\text{Br}_2) = 0.25$ torr, $P_0(\text{NO}) = 9.75$ torr

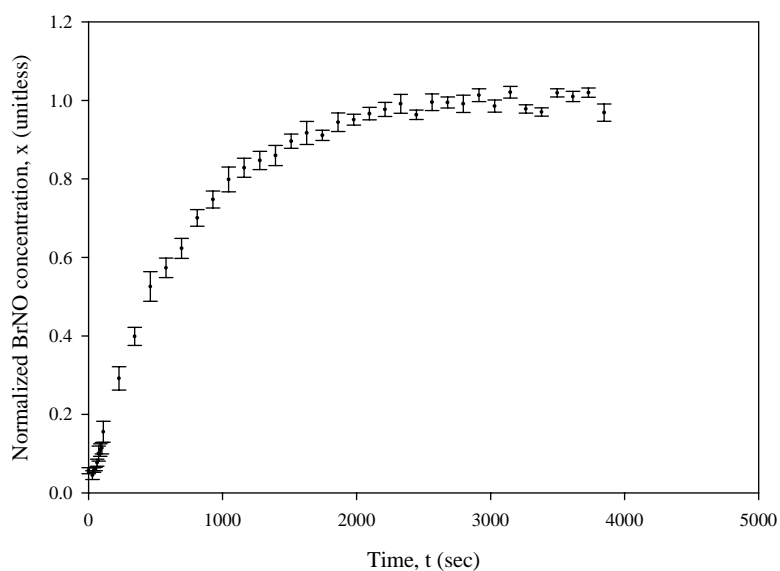


Figure 18. Normalized BrNO concentration, x , plotted as a function of time, t , for sample 6. $P_0(\text{Br}_2) = 0.30$ torr, $P_0(\text{NO}) = 9.70$ torr

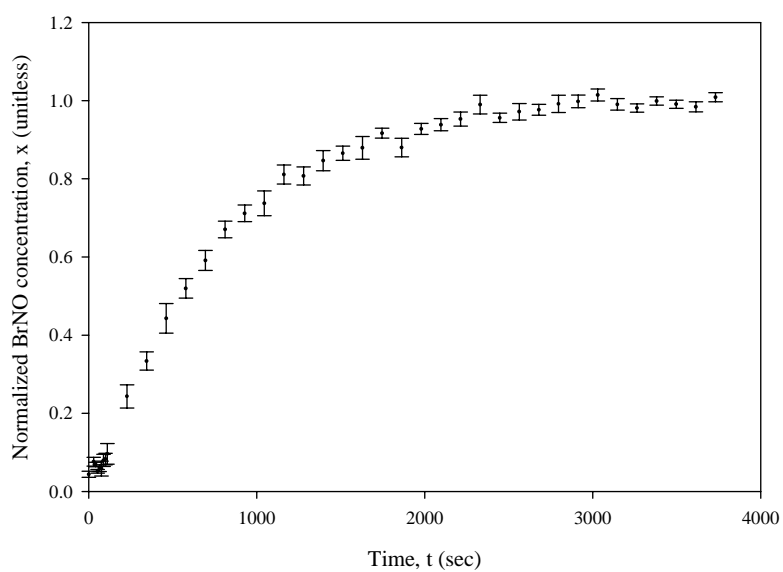


Figure 19. Normalized BrNO concentration, x , plotted as a function of time, t , for sample 7. $P_0(\text{Br}_2) = 0.25$ torr, $P_0(\text{NO}) = 9.75$ torr

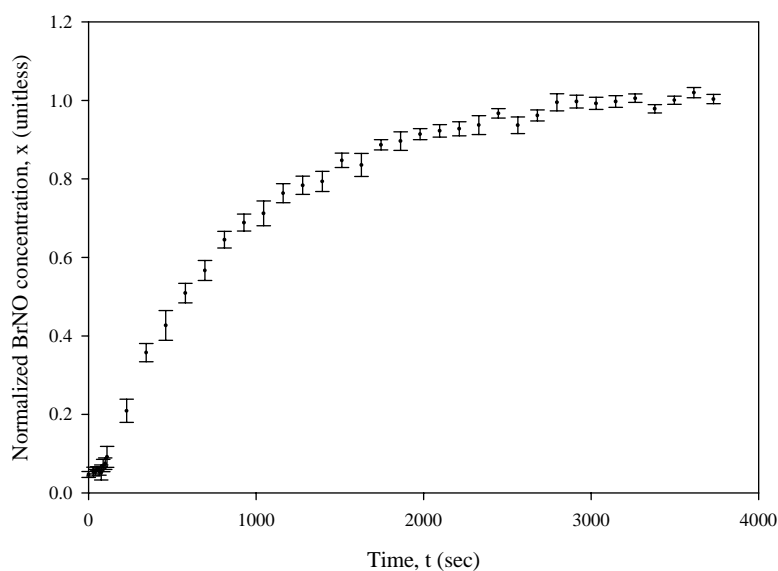


Figure 20. Normalized BrNO concentration, x , plotted as a function of time, t , for sample 8. $P_0(\text{Br}_2) = 0.23$ torr, $P_0(\text{NO}) = 9.77$ torr

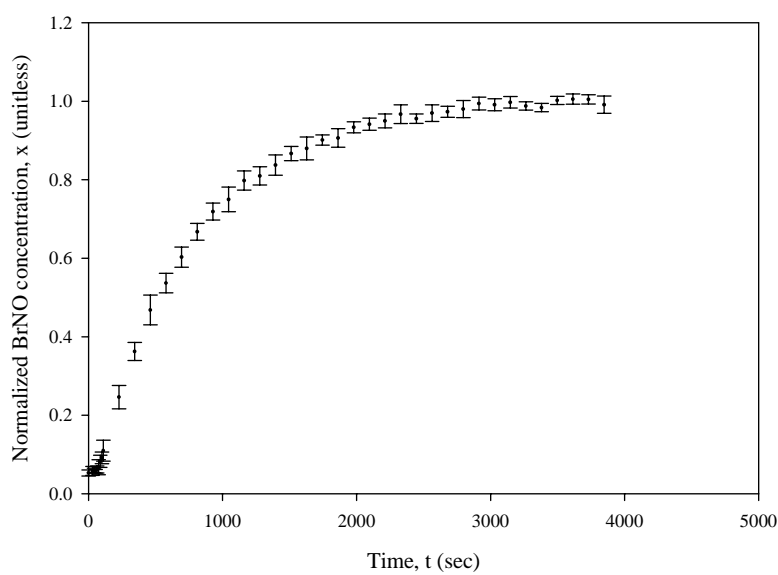


Figure 21. Normalized BrNO concentration, x , plotted as a function of time, t , for sample 9. $P_0(\text{Br}_2) = 0.28$ torr, $P_0(\text{NO}) = 9.72$ torr

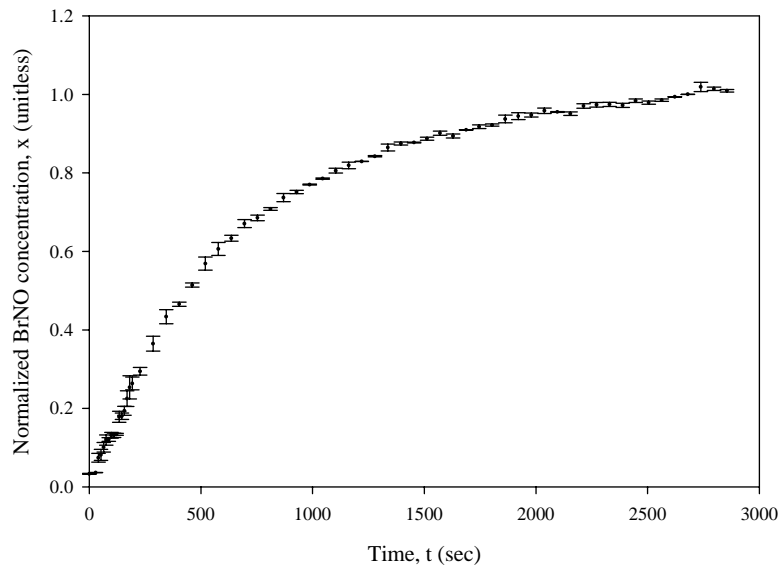


Figure 22. Normalized BrNO concentration, x , plotted as a function of time, t , for sample 10. $P_0(\text{Br}_2) = 0.30$ torr, $P_0(\text{NO}) = 9.70$ torr

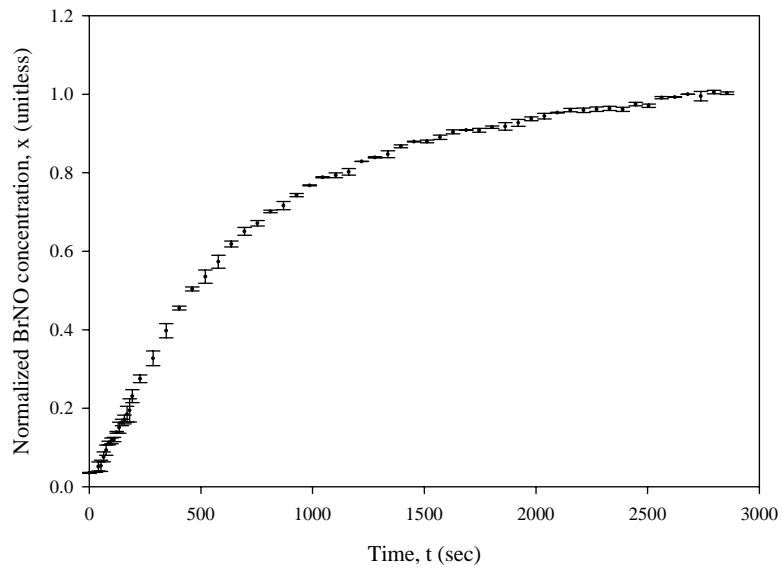


Figure 23. Normalized BrNO concentration, x , plotted as a function of time, t , for sample 11. $P_0(\text{Br}_2) = 0.30$ torr, $P_0(\text{NO}) = 9.70$ torr

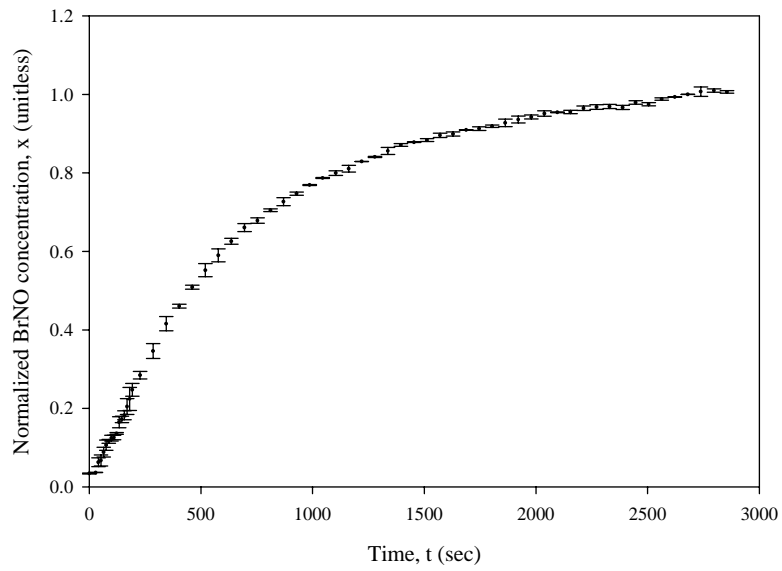


Figure 24. Normalized BrNO concentration, x , plotted as a function of time, t , for sample 12. $P_0(\text{Br}_2) = 0.25$ torr, $P_0(\text{NO}) = 9.75$ torr

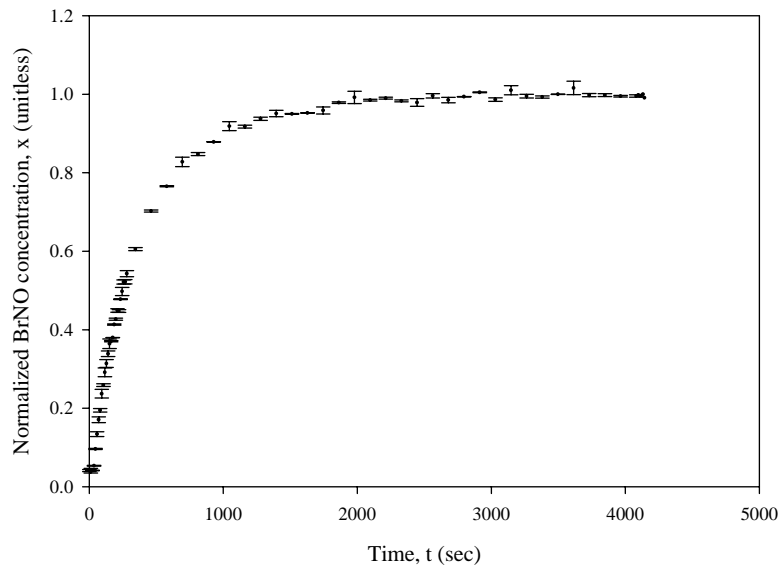


Figure 25. Normalized BrNO concentration, x , plotted as a function of time, t , for sample 13. $P_0(\text{Br}_2) = 0.35$ torr, $P_0(\text{NO}) = 9.65$ torr

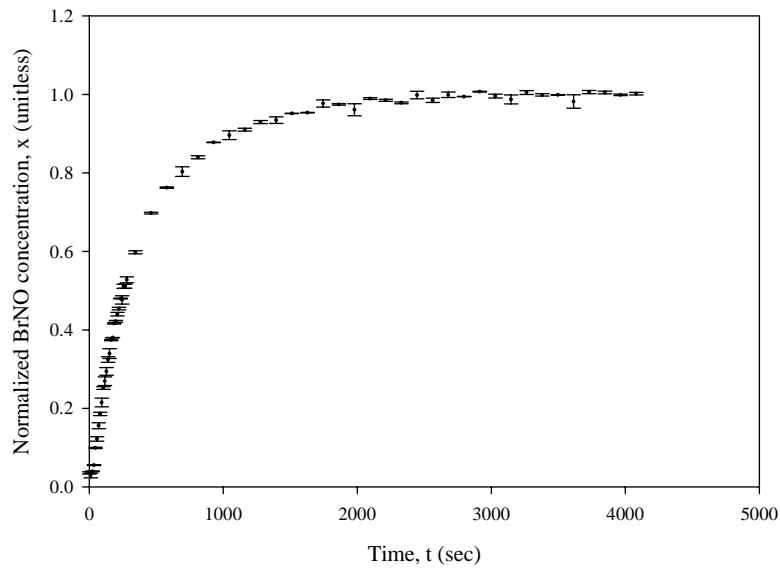


Figure 26. Normalized BrNO concentration, x , plotted as a function of time, t , for sample 14. $P_0(\text{Br}_2) = 0.35$ torr, $P_0(\text{NO}) = 9.65$ torr

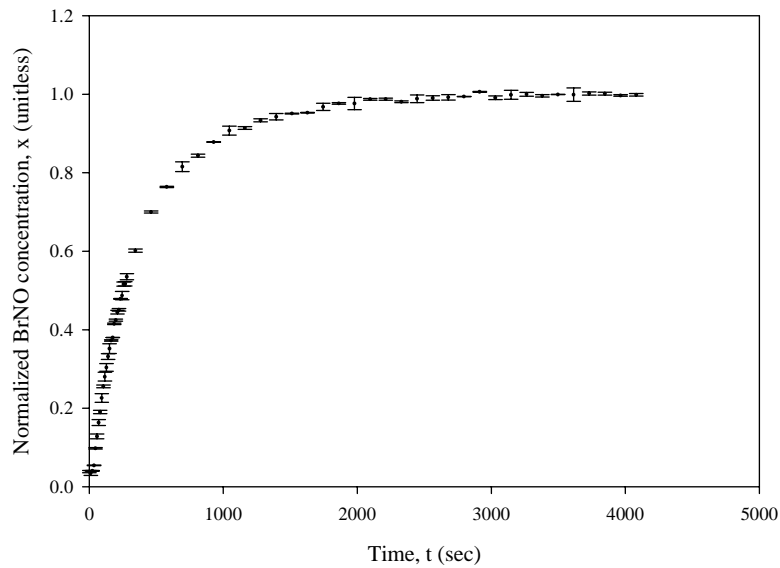


Figure 27. Normalized BrNO concentration, x , plotted as a function of time, t , for sample 15. $P_0(\text{Br}_2) = 0.35$ torr, $P_0(\text{NO}) = 9.65$ torr

Appendix C. Detailed Calculations of k_f , k_r , K_{eq} values

The following tables show the values that were used to determine k_f , k_r , and K_{eq} using first the third-order solution, equation (27), and then the first-order solution, equation (31). First, considering the situation where K_2 is the only fit parameter, using the values of $P_0(\text{Br}_2)$ and $P_0(\text{NO})$ that were calculated in Section IV and listed in Table 3, K_2 can be fit to equation (27) using Tablecurve. K_1 was calculated using K_2 , and a fixed value of α was determined from $[\text{NO}]_0$ and $[\text{Br}_2]_0$. Table 9 lists the parameters that were used to determine k_f and k_r with only K_2 as a fit parameter. Next, looking at the situation where both K_1 and K_2 were fit to the data using the third-order solution and α was again fixed, the values listed in Table 10 were used to determine k_f , k_r and K_{eq} . Finally, looking at the situation where $A=K_1\alpha^2$ was fit to the collected kinetics data using equation (31), the values listed in Table 11 were used to calculate k_f and k_r .

Table 9. Values used to determine k_f and k_r for case where K_2 was the only fit parameter

$f(\text{NO})_0$ (unitless)	$f(\text{Br}_2)_0$ (unitless)	n_{eq} (torr)	α (unitless)	$[\text{BrNO}]_{eq}$ (molecule/cm ³)	$[\text{NO}]_{eq}$ (molecule/cm ³)	$K_{eq}\text{BrNO}_{eq}$ (unitless)	K_1 (sec ⁻¹)	K_2 (sec ⁻¹)	K_2 Std Error (sec ⁻¹)	r^2
Pr = 10.0 torr, T=293 K, $K_{eq} = 6.71\text{E-}18$ cm ³ /molecule										
0.0925	0.9075	0.2912	0.717	1.78E+16	1.27E+16	0.119	8.79E-6	7.38E-5	6.80E-7	0.985
0.0920	0.9080	0.2913	0.717	1.77E+16	1.27E+16	0.118	8.72E-6	7.36E-5	5.66E-7	0.983
0.0922	0.9078	0.2913	0.717	1.77E+16	1.27E+16	0.119	8.40E-6	7.08E-5	3.27E-7	0.996
0.0920	0.9080	0.2913	0.717	1.77E+16	1.27E+16	0.118	7.71E-6	6.51E-5	4.52E-7	0.989
0.9750	0.0250	0.2381	19.477	1.57E+16	3.06E+17	0.105	6.95E-6	6.60E-5	1.53E-6	0.928
0.9700	0.0300	0.2827	16.158	1.86E+16	3.01E+17	0.125	1.02E-5	8.17E-5	2.79E-6	0.863
0.9750	0.0250	0.2381	19.477	1.57E+16	3.06E+17	0.105	7.90E-6	7.51E-5	1.81E-6	0.920
0.9770	0.0230	0.2199	21.216	1.45E+16	3.07E+17	0.097	6.79E-6	6.99E-5	1.88E-6	0.908
0.9720	0.0280	0.2650	17.343	1.75E+16	3.03E+17	0.117	8.48E-6	7.24E-5	1.39E-6	0.952
0.9700	0.0300	0.2827	16.158	1.86E+16	3.01E+17	0.125	1.11E-5	8.86E-5	1.22E-6	0.959
0.9700	0.0300	0.2827	16.158	1.86E+16	3.01E+17	0.125	1.11E-5	8.91E-5	9.79E-7	0.949
0.9750	0.0250	0.2381	19.477	1.57E+16	3.06E+17	0.105	8.54E-6	8.11E-5	1.34E-6	0.942
0.9650	0.0350	0.3262	13.791	2.15E+16	2.97E+17	0.144	1.56E-5	1.08E-4	2.54E-6	0.908
0.9650	0.0350	0.3262	13.791	2.15E+16	2.97E+17	0.144	1.74E-5	1.21E-4	2.63E-6	0.930
0.9650	0.0350	0.3262	13.791	2.15E+16	2.97E+17	0.144	1.70E-5	1.18E-4	2.98E-6	0.893

Table 10. Values used to determine k_f , k_r , and K_{eq} for case where K_1 and K_2 were the fit parameters

$f(\text{NO})_0$ (unitless)	$f(\text{Br}_2)_0$ (unitless)	n_{eq} (torr)	α (unitless)	$[\text{BrNO}]_{eq}$ (molecule/ cm^3)	$[\text{NO}]_{eq}$ (molecule/ cm^3)	K_1 (sec^{-1})	K_1 Std Error (sec^{-1})	K_2 (sec^{-1})	K_2 Std Error (sec^{-1})	r^2
P _T = 10.0 torr, T=293 K, K _{eq} = 6.71E-18 cm ³ /molecule										
0.0925	0.9075	0.2912	0.717	1.78E+16	1.27E+16	9.34E-6	4.93E-8	7.87E-5	4.23E-7	0.997
0.0920	0.9080	0.2913	0.717	1.77E+16	1.27E+16	8.56E-6	9.36E-8	7.22E-5	8.07E-7	0.984
0.0922	0.9078	0.2913	0.717	1.77E+16	1.27E+16	8.30E-6	4.77E-8	6.99E-5	4.08E-7	0.997
0.0920	0.9080	0.2913	0.717	1.77E+16	1.27E+16	7.38E-6	5.64E-8	6.23E-5	4.83E-7	0.993
0.9750	0.0250	0.2381	19.477	1.57E+16	3.06E+17	6.87E-6	2.74E-7	6.75E-5	4.71E-6	0.928
0.9700	0.0300	0.2827	16.158	1.86E+16	3.01E+17	1.07E-5	6.16E-7	7.49E-5	6.65E-6	0.865
0.9750	0.0250	0.2381	19.477	1.57E+16	3.06E+17	7.95E-6	3.41E-7	7.41E-5	6.00E-6	0.920
0.9770	0.0230	0.2199	21.216	1.45E+16	3.07E+17	6.84E-6	3.15E-7	6.88E-5	5.86E-6	0.908
0.9720	0.0280	0.2650	17.343	1.75E+16	3.03E+17	8.59E-6	2.76E-7	7.06E-5	3.57E-6	0.952
0.9700	0.0300	0.2827	16.158	1.86E+16	3.01E+17	1.13E-5	2.28E-7	8.56E-5	2.28E-6	0.960
0.9700	0.0300	0.2827	16.158	1.86E+16	3.01E+17	1.20E-5	3.23E-7	8.01E-5	2.94E-6	0.941
0.9750	0.0250	0.2381	19.477	1.57E+16	3.06E+17	8.11E-6	2.27E-7	8.87E-5	3.99E-6	0.944
0.9650	0.0350	0.3262	13.791	2.15E+16	2.97E+17	1.54E-5	6.42E-7	1.13E-4	9.05E-6	0.908
0.9650	0.0350	0.3262	13.791	2.15E+16	2.97E+17	1.73E-5	6.25E-7	1.23E-4	8.34E-6	0.930
0.9650	0.0350	0.3262	13.791	2.15E+16	2.97E+17	1.72E-5	7.70E-7	1.14E-4	1.04E-5	0.893

Table 11. Values used to determine k_f and k_r for case where $K_1\alpha^2$ was the fit parameter

$f_{\text{NO}0}$ (unitless)	$f_{\text{Br}20}$ (unitless)	n_{eq} (torr)	$[\text{BrNO}]_{eq}$ (molecule/ cm^3)	$[\text{NO}]_{eq}$ (molecule/ cm^3)	$K_1\alpha^2$ (sec^{-1})	$K_1\alpha^2$ Std Error (sec^{-1})	α (unitless)	K_1 (sec^{-1})	K_2 (sec^{-1})	r^2
P _T = 10.0 torr, T=293 K, K _{eq} = 6.71E-18 cm ³ /molecule										
0.9750	0.0250	0.2381	1.57E+16	3.06E+17	2.66E-3	3.54E-5	19.477	7.00E-6	6.65E-5	0.997
0.9700	0.0300	0.2827	1.86E+16	3.01E+17	2.94E-3	3.51E-5	16.158	1.13E-5	9.02E-5	0.998
0.9750	0.0250	0.2381	1.57E+16	3.06E+17	2.65E-3	3.21E-5	19.477	6.97E-6	6.63E-5	0.997
0.9770	0.0230	0.2199	1.45E+16	3.07E+17	2.46E-3	3.19E-5	21.216	5.47E-6	5.63E-5	0.997
0.9720	0.0280	0.2650	1.75E+16	3.03E+17	2.67E-3	2.50E-5	17.343	8.86E-6	7.57E-5	0.998
0.9700	0.0300	0.2827	1.86E+16	3.01E+17	3.03E-3	2.00E-5	16.158	1.16E-5	9.28E-5	0.998
0.9700	0.0300	0.2827	1.86E+16	3.01E+17	2.96E-3	1.85E-5	16.158	1.13E-5	9.06E-5	0.999
0.9750	0.0250	0.2381	1.57E+16	3.06E+17	2.99E-3	2.00E-5	19.477	7.88E-6	7.49E-5	0.999
0.9650	0.0350	0.3262	2.15E+16	2.97E+17	5.28E-3	7.00E-5	13.791	2.77E-5	1.92E-4	0.997
0.9650	0.0350	0.3262	2.15E+16	2.97E+17	5.14E-3	7.40E-5	13.791	2.70E-5	1.87E-4	0.997
0.9650	0.0350	0.3262	2.15E+16	2.97E+17	5.21E-3	6.80E-5	13.791	2.74E-5	1.90E-4	0.997

Bibliography

1. ABB Bomem, Inc. *Bomem GRAMS/32 collect driver User's Guide*. Rev 1-1, 1999.
2. ABB Bomem Inc. *FT-IR Reference Manual*. Rev 1-1, 2001.
3. Degli Esposti, C., et al. "High resolution Fourier Transform Spectroscopy of the ν_1 Fundamental Band of Nitrosyl Bromide," *Chemical Physics Letters*, 214: 531-535 (November 1993).
4. Godfrey, Patrick. *Kinetics and Spectroscopy of BrNO*. PhD dissertation, Air Force Institute of Technology, Wright-Patterson AFB, OH, 1997.
5. Green, Don W, editor. *Perry's Chemical Engineers' Handbook* (7th Edition). New York: McGraw Hill, 1997.
6. Hawks, Michael. *Infrared Fluorescence Studies of Electronic-to-Vibronal Energy Transfer in a $Br_2:NO$ System*. Master's Thesis, Air Force Institute of Technology, Wright-Patterson AFB, OH. 1993.
7. Hippler, H., et al. "Flash Photolysis Study of the NO-Catalyzed Recombination of Bromine Atoms," *International Journal of Chemical Physics*, 10:155-169 (1978).
8. Hisatsune, I.C. and Leo Zafonte. "A Kinetic Study of Some Third-Order Reactions of Nitric Oxide," *Journal of Physical Chemistry*, 73: 2980-2989 (September 1969).
9. Hollas, J Micheal. *Modern Spectroscopy*. West Sussex, England: John Wiley & Sons Ltd, 1996.
10. Houel, N. and H. Van Den Bergh. "BrNO – Thermodynamic Properties, the Ultraviolet/Vis Spectrum, and the Kinetics of Its Formation," *International Journal of Chemical Kinetics*, 9: 867-874 (1977).
11. Johnson, Ray. *Excited Atomic Bromine Energy Transfer and Quenching Mechanisms*. PhD Dissertation, Air Force Institute of Technology, Wright-Patterson AFB, OH. 1993.
12. Kee, Patrick. Personal communication, 2003.
13. Laane, J, et al. "Vibrational Spectra and Force Constants for the Isotopic Species of Nitrosyl Bromide," *Journal of Molecular Spectroscopy*, 30:485-497 (1969).
14. Laidler, Keith J. *Chemical Kinetics*. New York: McGraw-Hill, 1965.
15. Perram, Glen. Personal communication, 2004.
16. Spectra Physics. *Millenia VI J User Manual*. 2001.
17. Weast, Robert C., editor. *CRC Handbook of Chemistry and Physics* (56th Edition). Cleveland OH: CRC Press, 1975.

REPORT DOCUMENTATION PAGE

*Form Approved
OMB No. 074-0188*

The public reporting burden for this collection of information is estimated to average 1 hour per response, including the time for reviewing instructions, searching existing data sources, gathering and maintaining the data needed, and completing and reviewing the collection of information. Send comments regarding this burden estimate or any other aspect of the collection of information, including suggestions for reducing this burden to Department of Defense, Washington Headquarters Services, Directorate for Information Operations and Reports (0704-0188), 1215 Jefferson Davis Highway, Suite 1204, Arlington, VA 22202-4302. Respondents should be aware that notwithstanding any other provision of law, no person shall be subject to a penalty for failing to comply with a collection of information if it does not display a currently valid OMB control number.

PLEASE DO NOT RETURN YOUR FORM TO THE ABOVE ADDRESS.

1. REPORT DATE (DD-MM-YYYY) 01-12-2004		2. REPORT TYPE Master's Thesis		3. DATES COVERED (From - To) Apr 2003 - Nov 2004	
4. TITLE AND SUBTITLE The Kinetics Following Photolysis of Nitrosyl Bromide				5a. CONTRACT NUMBER	
				5b. GRANT NUMBER	
				5c. PROGRAM ELEMENT NUMBER	
6. AUTHOR(S) Mahoney, Lori, A., Civilian				5d. PROJECT NUMBER	
				5e. TASK NUMBER	
				5f. WORK UNIT NUMBER	
7. PERFORMING ORGANIZATION NAMES(S) AND ADDRESS(S) Air Force Institute of Technology Graduate School of Engineering and Management (AFIT/EN) 2950 Hobson Way WPAFB OH 45433-7765				8. PERFORMING ORGANIZATION REPORT NUMBER AFIT/GAP/ENP/04-07	
9. SPONSORING/MONITORING AGENCY NAME(S) AND ADDRESS(ES) N/A				10. SPONSOR/MONITOR'S ACRONYM(S)	
				11. SPONSOR/MONITOR'S REPORT NUMBER(S)	
12. DISTRIBUTION/AVAILABILITY STATEMENT APPROVED FOR PUBLIC RELEASE; DISTRIBUTION UNLIMITED.					
13. SUPPLEMENTARY NOTES					
14. ABSTRACT One candidate for the development of a tunable laser in the mid-infrared for use as a defensive countermeasure exploits the NO transition at 5.4 μm. The difficulty with this laser is that when Br ₂ and NO are present in a mixture, nitrosyl bromide (BrNO) is also created. The absorption bands present in BrNO complicate the design of such a laser. This thesis determines the forward and reverse rate constants of the reaction of Br ₂ and NO to form BrNO following the photolysis BrNO at low pressure using Fourier Transform infrared absorption spectroscopy, where samples contain either Br ₂ or NO in excess. The use of Br ₂ versus NO as the excess reagent has an effect on which mechanism can be used to describe the reaction, but does not affect the reaction rate constants. When NO is the excess reagent, the reaction obeys pseudo first-order kinetics, but in both cases, third-order kinetics accurately describe the Br ₂ + 2NO ↔ 2BrNO reaction giving a forward reaction rate constant of k _f = 1.56 ± 0.20 x 10 ⁻³⁸ cm ⁶ /molecule ² -s at 293 ± 1 K. The reverse rate constant was calculated as k _r = 2.29 ± 0.33 x 10 ⁻²¹ cm ³ /molecule-s and the equilibrium constant as K _{eq} = 171 ± 13 atm ⁻¹ . This result is consistent with previous results.					
15. SUBJECT TERMS Kinetics, Reaction Kinetics, Reaction Rate, Nitric Oxide, Bromine, Bromine Compounds, Nitrosyl Bromide, Chemical Equilibrium, Absorption, Infrared Absorption, Fourier Transform Spectroscopy					
16. SECURITY CLASSIFICATION OF:		17. LIMITATION OF ABSTRACT UU	18. NUMBER OF PAGES 56	19a. NAME OF RESPONSIBLE PERSON Glen P. Perram (ENP)	
REPORT U	ABSTRACT U			19b. TELEPHONE NUMBER (Include area code) (937) 255-3636, ext 4504; e-mail: Glen.Perram@afit.edu	

Standard Form 298 (Rev. 8-98)

Prescribed by ANSI Std. Z39-18